RESEARCH ARTICLE

WILEY *genesis*
The Journal of Genetics and Development

Specific and spatial labeling of *P0-Cre* versus *Wnt1-Cre* in cranial neural crest in early mouse embryos

Guiqian Chen[1] | Mohamed Ishan[1] | Jingwen Yang[2] | Satoshi Kishigami[3] | Tomokazu Fukuda[3] | Greg Scott[4] | Manas K. Ray[4] | Chenming Sun[5] | Shi-You Chen[5] | Yoshihiro Komatsu[2,3,6] | Yuji Mishina[2,3,4] | Hong-Xiang Liu[1]

[1]Regenerative Bioscience Center, Department of Animal and Dairy Science, College of Agricultural and Environmental Sciences, University of Georgia, Athens, Georgia 30602

[2]Department of Biologic and Materials Sciences, School of Dentistry, University of Michigan, Ann Arbor, Michigan 48109

[3]Reproductive and Developmental Biology Laboratory, National Institute of Environmental Health Sciences, Research Triangle Park, North Carolina, 27709

[4]Knockout Core, National Institute of Environmental Health Sciences, Research Triangle Park, North Carolina, 27709

[5]Department of Physiology and Pharmacology, College of Veterinary Medicine, University of Georgia, Athens, Georgia 30602

[6]Department of Pediatrics, The University of Texas Medical School at Houston, Houston, Texas 77030

Correspondence
Yuji Mishina, Department of Biologic and Materials Sciences, School of Dentistry, University of Michigan, Ann Arbor, Michigan 48109.
Email: mishina@umich.edu and Hong-Xiang Liu, Regenerative Bioscience Center, Department of Animal and Dairy Science, College of Agricultural and Environmental Sciences, University of Georgia, Athens, Georgia 30602.
Email: lhx@uga.edu

Present address
Satoshi Kishigami, Department of Biotechnology, Faculty of Life and Environmental Sciences University of Yamanashi, Japan and Tomokazu Fukuda, Iwate University, Faculty of Science and Engineering, Morioka, Iwate, Japan

Funding information
NIH, Grant numbers: R01DE020843, ES071003-11, R01DC012308

Abstract

P0-Cre and *Wnt1-Cre* mouse lines have been widely used in combination with loxP-flanked mice to label and genetically modify neural crest (NC) cells and their derivatives. *Wnt1-Cre* has been regarded as the gold standard and there have been concerns about the specificity of *P0-Cre* because it is not clear about the timing and spatial distribution of the *P0-Cre* transgene in labeling NC cells at early embryonic stages. We re-visited *P0-Cre* and *Wnt1-Cre* models in the labeling of NC cells in early mouse embryos with a focus on cranial NC. We found that *R26-lacZ* Cre reporter responded to Cre activity more reliably than *CAAG-lacZ* Cre reporter during early embryogenesis. Cre immunosignals in *P0-Cre* and reporter (*lacZ* and *RFP*) activity in *P0-Cre/R26-lacZ* and *P0-Cre/R26-RFP* embryos was detected in the cranial NC and notochord regions in E8.0–9.5 (4–19 somites) embryos. *P0-Cre* transgene expression was observed in migrating NC cells and was more extensive in the forebrain and hindbrain but not apparent in the midbrain. Differences in the Cre distribution patterns of *P0-Cre* and *Wnt1-Cre* were profound in the midbrain and hindbrain regions, that is, extensive in the midbrain of *Wnt1-Cre* and in the hindbrain of *P0-Cre* embryos. The difference between *P0-Cre* and *Wnt1-Cre* in labeling cranial NC may provide a better explanation of the differential distributions of their NC derivatives and of the phenotypes caused by Cre-driven genetic modifications.

KEYWORDS
derivation, lineage tracing, mouse, neural crest, Wnt1-Cre, P0-Cre

1 | INTRODUCTION

Neural crest (NC) is a multipotent cell population derived from the lateral ridges of the neural plate in early vertebrate embryos (Leikola, 1976; Trainor, 2015). After delamination from the neural folds, NC cells migrate ventrally and extensively, giving rise to a wide variety of differentiated cell types, for example, neurons, glia, bone, cartilage, and connective tissue of the head (Bronner-Fraser, 2004; Crane and Trainor, 2006; Meulemans and Bronner-Fraser, 2004; Munoz and Trainor, 2015; Trainor, 2005b). Labeling and tracking NC have been essential for understanding the NC contribution to different tissue and cell types, which is fundamental for organogenesis.

Recently, cell lineage tracing using NC-specific promoter driven *Cre* transgenic mouse lines in combination with *Cre* reporter mouse lines has facilitated genetic marking of NC cells and their derivatives. Multiple *Cre* transgenic mouse lines have been generated using a NC marker gene promoter, for example, *Wnt1-Cre* (Echelard, Vassileva, & McMahon, 1994; Jiang, Iseki, Maxson, Sucov, & Morriss-Kay, 2002; McMahon, Joyner, Bradley, & McMahon, 1992), *P0-Cre* (Wang, Komatsu, & Mishina, 2011; Yamauchi et al., 1999; Zhang, Marsh, Ratner, & Brackenbury, 1995), *Dhh-Cre* (Gershon et al., 2009; Wang, Kumar, Mitsios, Slevin, & Kumar, 2007), *Pax3-Cre* (Jarad and Miner, 2009), *HtPA-Cre* (Lee et al., 2013), *Sox10-Cre* (Simon, Lickert, Gotz, & Dimou, 2012), *Mef2c-F10N-Cre* (Aoto et al., 2015). Use of these models has yielded new data pertaining to NC cell specifications in mice, for example, distinct genesis of skin-derived precursors in craniofacial and dorsal skin from NC and mesoderm, respectively (Jinno et al., 2010), NC and placodal derivation of the otic vesicle (Freyer, Aggarwal, & Morrow, 2011), a dual origin of sensory organs that include olfactory epithelium (Katoh et al., 2011) and taste bud cells (Boggs et al., 2016; Liu, Komatsu, Mishina, & Mistretta, 2012), and a dual origin of tooth bud epithelium (Wang et al., 2011).

However, variations/discrepancies in the different models that label NC cell lineage have been reported, such as in tooth (Wang et al., 2011); olfactory epithelium (Suzuki, Yoshizaki, Kobayashi, & Osumi, 2013); heart (Cavanaugh, Huang, & Chen, 2015; Milgrom-Hoffman et al., 2014; Nakamura, Colbert, & Robbins, 2006; Tomita et al., 2005), and taste organs (Boggs et al., 2016; Liu et al., 2012). In comparative studies on NC contributions to specific lineages, the *Wnt1-Cre* and *P0-Cre* lines have been widely used (Katoh et al., 2011; Liu et al., 2012; Morikawa et al., 2009; Nagoshi et al., 2008, Nagoshi et al., 2011; Nakamura et al., 2006; Yoshida et al., 2006; Yoshida et al., 2008). *Wnt1-Cre* has been regarded as the gold standard for NC lineage, however, *Wnt1-Cre* also labels cells in the neural tube that makes researchers question the specificity of this line and other models when a difference is observed compared to *Wnt1-Cre* (Trainor, 2005a). In fact, a difference between *Wnt1-Cre* and *P0-Cre* in labeling NC has been found in multiple organs (Freem et al., 2010; Kawakami et al., 2011; Lewis et al., 2013; Liu et al., 2012; Wang et al., 2011). In contrast to *Wnt1-Cre*, which has been reported to trace NC cells as early as E8.5 using a *ROSA26* (hereafter, *R26-lacZ*) Cre reporter in mice (Chai et al., 2000; Ikeya et al., 1997; Jiang et al., 2002; McMahon et al., 1992), *P0-Cre* has been reported to label NC derivatives at stages later than E9.0 using *CAAG-CAT-lacZ* (hereafter, *CAAG-lacZ*) as a reporter system (Yamauchi et al., 1999). Although *in situ* hybridization for *P0-Cre* transgene expression was performed (Yamauchi et al., 1999), there is no detailed information available regarding the labeling of *P0-Cre* in NC cells at early stages.

In the present study, the expression of two commonly used reporter transgenes, *CAAG-lacZ* and *R26-lacZ*, were compared in early embryos, and we found that DNA recombination was not consistent in the *CAAG-lacZ* reporter when driven by *Meox2-Cre* in early embryos. To further evaluate the timing, specificity and spatial distribution of *P0-*

Cre and *Wnt1-Cre* activity, we used the *R26-lacZ* and *R26-tdTomato* (*R26-RFP*) reporters and carried out immunoreactions for Cre. Subsequently, we thoroughly compared the presence of Cre recombinase in pre- and post-migratory NC cells in *P0-Cre* and *Wnt1-Cre* embryos. Our data indicate that the *P0-Cre* transgene expression is specifically distributed in migrating cranial NC in addition to the notochord, and Cre immunosignals were especially extensive in the forebrain and hindbrain regions. In contrast, *Wnt1-Cre* transgene expression was obvious in forebrain and midbrain NC cells but was sparse in migrating NC in the hindbrain regions.

2 | MATERIALS AND METHODS

2.1 | Animals

Animals were maintained and used in compliance with institutional animal care protocols of the University of Georgia, the University of Michigan and the National Institute of Environmental Health, and in accordance with the National Institutes of Health Guidelines for Care and Use of Animals in research.

Mice carrying Cre recombinase driven by the protein zero (P0) promoter (*P0-Cre* mouse, *C57BL/6J-Tg(P0-Cre)94Imeg* (ID 148)), were provided by CARD, Kumamoto University, Japan (Yamauchi et al., 1999) and were mated with C57BL/6 wild type (WT) or *Cre*-reporter mice *R26-lacZ* (Soriano, 1999) or *ZEG (LacZ/EGFP)* (Novak et al., 2000) or *R26-tdTomato* (RFP) (B6.Cg-*Gt(ROSA)26Sor$^{tm14(CAG-tdTomato)Hze}$/J*, Jackson Lab, Stock #007914) to generate *P0-Cre/WT*, *P0-Cre/R26-lacZ*, *P0-Cre/ZEG*, and *P0-Cre/RFP* mice. *Meox2-Cre* mice, which express *Cre* in the epiblast from E5.5 (Tallquist and Soriano, 2000), were also bred with *R26-lacZ* or *Cre*-reporter *CAAG-lacZ* mouse line (Sakai and Miyazaki, 1997). *Wnt1-Cre* mice (*B6.Cg-Tg(Wnt1-cre)11Rth Tg(Wnt1-GAL4)11Rth/J*, Jackson Lab, Stock# 009107) were bred with C57BL/6 WT or *Cre*-reporter mice *R26-lacZ* (Soriano, 1999) or *R26-RFP* to generate *Wnt1-Cre/WT* or *Wnt1-Cre/R26-lacZ* or *Wnt1-Cre/RFP*. *R26-lacZ* reporter mice were maintained on a mixed background of C57BL/6 (majority) and 129S6.

2.2 | Tissue collection

Timed pregnant mice were euthanized using CO_2 followed by cervical dislocation to ensure death. The uterus with embryos was removed and embryos were retrieved under a microscope. The tissues were further dissected and processed for analysis, as described below.

Embryos from *P0-Cre* mice were harvested at embryonic day (E) 8.0, E8.5, E9.5, and E10.5. Newborn *P0-Cre/ZEG* mice were harvested immediately after birth. *Meox2-Cre* mouse embryos carrying a *Cre*-reporter were obtained from E6.5 to E11.5. *Wnt1-Cre* mouse embryos were collected at E8.0–E8.5. Noon of the day on which the dam was positive for vaginal plug was designated as E0.5. The stages of these embryos were confirmed by comparing the sizes and morphologies of multiple organs. The number of pairs of somites was counted under a microscope at the time of dissection.

2.3 | Genotyping

Specific primers were used to genotype the mice. Primers A (5′-CTC GTG ATC TGC AAC TCC AGTC-3′) and B (5′-GAG ACT AGT GAG ACG TGC TACT-3′) were used to amplify fragments from the un-recombined *R26-lacZ* reporter allele (∼550 bp). Primers A and C (5′-TGT GAG CGA GTA GTA ACA ACC-3′) were used to detect the Cre-recombined allele (∼680 bp). Primers E (5′-CAG TCA GTT GCT CAA TGT ACC-3′) and F (5′-ACT GGT GAA ACT CAC CCA-3′) were used to amplify fragments from the un-recombined *CAAG-lacZ* allele (∼450 bp), whereas primers D (5′-GTG CTG GTT ATT GTG CTG TCTC-3′) and C were used to detect *Cre*-dependent deletion of the floxed region (∼680 bp). To detect a *Cre* transgene, Cre1 (5′-GGA CAT GTT CGG GAT CGC CAG GCG-3′) and Cre2 (5′-GCA TAA CCA GTG AAA CAG CAT TGC TG-3′) primers were used.

2.4 | X-gal staining

After dissection, the embryos were fixed with 4% paraformaldehyde for 5 min at 4°C, and washed three times with 0.1 M sodium phosphate buffer (PBS, pH 7.5), then stained with 1 mg mL^{-1} of 5-bromo-4-chloro-3-indolyl-beta-D-galactoside (X-gal, Sigma, Cat# B-4252) in 0.1 M PBS, 0.1% sodium deoxycholate, 0.2% Nonidet P-40, 2 mM magnesium chloride, 5 mM potassium ferricyanide, and 5 mM potassium ferrocyanide at 37°C.

2.5 | Immunohistochemistry

Embryos were fixed with 4% paraformaldehyde in 0.1 M PBS (pH 7.3) for 2 hr at 4°C, rinsed in PBS and then infiltrated with 20–30% sucrose prior to embedding in OCT/Tissue Tek (Sakura Finetek). Serial sections were cut at 10-μm thickness. Sections were air dried, rehydrated and blocked with 10% normal donkey serum for 1 hr at room temperature. Primary antibodies against the following proteins were applied: Cre recombinase (1:500, MAB3120, EMD Millipore, Billerica, MA), FOXA2 (1:500, 07-633, EMD Millipore, Billerica, MA), GFP (1:100, ab13970, abcam, Cambridge, MA), p75 (1:200, sc-6188, Santa Cruz Biotechnology, Dallas, TX), SOX9 (1:1000, sc-20095, Santa Cruz Biotechnology, Dallas, TX; 1:1000, ab185966, abcam, Cambridge, MA). Primary antibodies were diluted with 0.1 M PBS that contained 0.3% Triton X-100 and 1% normal donkey serum. After incubation with primary antibody overnight at 4°C, sections were washed three times with 0.1 M PBS, and then incubated with secondary antibodies that were conjugated with Alexa Fluor 488, Alexa Fluor 546 or 647 (1:500, Invitrogen) for 1 hr at room temperature in 0.1 M PBS containing 0.3% Triton X-100 and 1% normal donkey serum. Sections were counterstained with DAPI solution for 5–10 min to visualize nuclei and were then rinsed in PBS. After air drying, the slides were mounted with ProLong® Gold antifade medium (Invitrogen, Eugene, OR), and the sections were examined thoroughly using a light microscope (EVOS FL, Life Technologies). Colocalization of different immunosignals was confirmed and photographed using a laser-scanning confocal microscope (Zeiss LSM 710).

To confirm the specificity of immunosignals, slides without the addition of primary antibodies were used as negative staining controls for all immunostainings in the present study. For determining specificity of Cre immuno-labeling, Cre negative littermate embryos were sectioned and immunoreacted with the same concentration of primary and secondary antibodies. Additionally, Western blotting was conducted using E9.5 *P0-Cre* embryos (Cre$^+$ embryos and Cre$^-$ littermate control) to further investigate the specificity of antibodies against Cre recombinase (1:5000, MAB3120, EMD Millipore, Billerica, MA). A ubiquitously expressed protein, IκB kinase complex associated protein (IKAP) (1:5000, sc-8336, Santa Cruz Biotechnology) was used as a loading control. Equal amounts of protein were used for electrophoresis in sodium dodecyl sulfate-polyacrylamide gel and transferred to a nitrocellulose membrane. Procedures for blocking and antibody probing were performed as described (Li et al., 2011). A single band at the expected molecular weight was detected in a genotype-dependent manner with the Cre antibody (Supporting Information Figure 1).

3 | RESULTS

3.1 | *Meox2-cre* driven *R26-lacZ* reporter expression emerges earlier and is more consistent than *CAAG-lacZ*

ROSA26 Cre reporter (hereafter, *R26-lacZ*) and *CAAG-CAT-lacZ* Cre reporter (hereafter, *CAAG-lacZ*) mice have been widely used for cell fate mapping. First, we compared the reporter sensitivity of these two lines at early embryo stages (E6.5–E11.5, Figure 1) using the *Meox2-Cre* transgenic line in which Cre activity emerges as early as E5.5 in the epiblast (Tallquist and Soriano, 2000). In *Meox2-Cre/R26-lacZ* mice, X-gal staining of whole embryos showed that signals appeared in the earliest stage examined (E6.5) and that labeled cells were extensively distributed in the whole embryos throughout all the stages examined (Figure 1a) similarly to the previous report (Tallquist and Soriano, 2000). In contrast, β-galactosidase (β-gal) activity in *Meox2-Cre/CAAG-lacZ* embryos was not detected until E7.5 (*n* = 5 or more for each stage). Weak signals were detected in the cardiac region at E8.5 (2/5) and in the somites and heart region at E9.5 (2/5) (Figure 1b), but were not apparent in head and other tissues in the trunk regions. At E10.5 and E11.5 (6/6 for each stage), the distribution of *CAAG-lacZ* expression in *Meox2-Cre/CAAG-lacZ* embryos was similar to that of *Meox2-Cre/R26-lacZ* throughout the entire embryo (Figure 1b).

To examine whether the discrepancy between *Meox2-Cre* driven *R26-lacZ* and *CAAG-lacZ* reporter activity was caused by DNA recombination efficiency, promoter silencing, or both, specific primers were designed to detect unrecombined and recombined reporter alleles (Figure 1c,d). A fragment of ∼550 bp was produced using primers A and B to detect the un-recombined *R26-lacZ* alleles. A Cre-recombined *R26-lacZ* allele was detected using primers A and C, and the product was approximately 680 bp (Figure 1c). For the *CAAG-lacZ* reporter system, primers E and F were used to generate an ∼450 bp fragment from unrecombined allele whereas primers D and C produced an ∼680 bp fragment from the Cre-mediated allele (Figure 1d). Both *Cre* transgenes
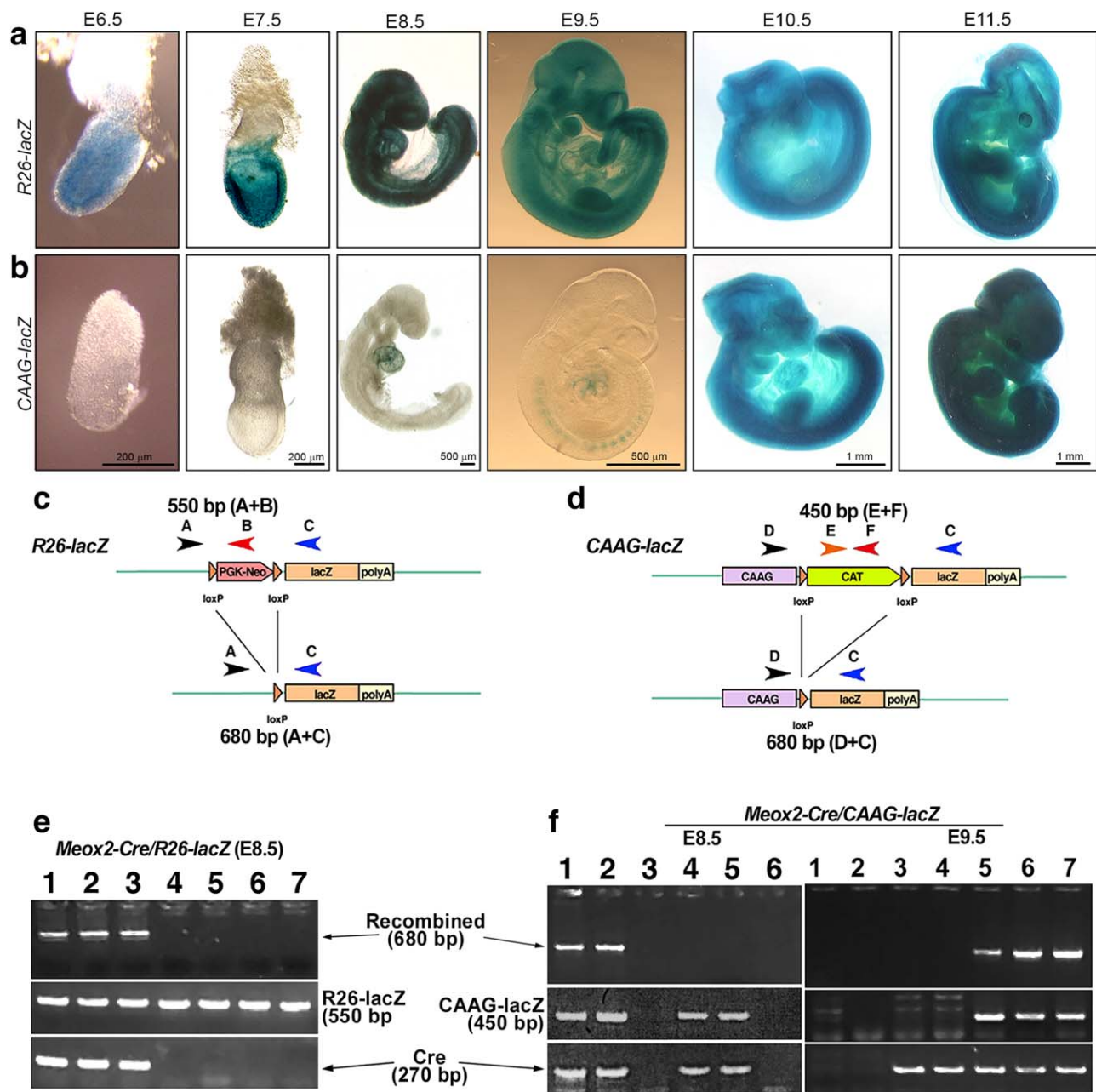
FIGURE 1 (a,b): X-Gal visualization of the *lacZ* gene product β-galactosidase in *R26-lacZ* (a) and *CAAG-lacZ* (b) reporters driven by *Meox2-Cre* at different mouse embryonic stages. β-gal positive signals (blue) were ubiquitous in *R26-lacZ* embryos at all stages examined from E6.5 to E11.5. In the *CAAG-lacZ* embryos, positive signals were not detected until E9.5 and the embryos were not ubiquitously labeled until E10.5. At least two litters were dissected to collect 5 or more embryos at each stage. Scale bars in (b) also apply to (a). (c–f): Schematic diagrams (c,d) and representative genotyping data (e,f) of the *R26-lacZ* (c,e) and *CAAG-lacZ* (d,f) reporter systems. *Meox2-Cre* was used to drive reporter gene activation. In the E8.5 *Meox2-Cre/R26R-lacZ* embryos, Cre recombined bands were consistently detected when both *R26-lacZ* and *Cre* were present (e, lanes 1–3). However, recombined bands were detected in only 50% of the E8.5 *Meox2-Cre/CAAG-lacZ* embryos (f, lane 1–2). Although both *CAAG-lacZ* and *Cre* were present, Cre recombination products were not detected in half of the E8.5 embryos (f, E8.5, lane 4–5). At E9.5, the detection of Cre recombination products was coincident with the presence of both *CAAG-lacZ* and *Cre* (f, E9.5, lane 5–7). *n* = 5 or more for each stage and genotype

were detected using primers Cre1 and Cre2 to generate an 270 bp fragment (Figure 1c,d).

In E8.5 *Meox2-Cre/R26-lacZ* embryos, the recombined allele was reliably detected when both *Cre* and *R26-lacZ* transgenes were present

(Figure 1e, lane 1–3) compared to the absence of bands without *Cre* transgene (Figure 1e, lane 4–7). In contrast, in *Meox2-Cre/CAAG-lacZ* mice only half of the double transgenic embryos showed detectable recombined allele at E8.5 (Figure 1f, E8.5, lane 1–2 vs. 4–5). The

FIGURE 2 Whole mount X-Gal visualization of the *lacZ* gene product β-galactosidase in *P0-Cre/R26-lacZ* mouse embryos at different somite (s) stages (E8-E9, 4s-26s). The somite number is indicated in each panel. At the 4-somite stage, β-gal positive signals (blue) emerged (a top, a', arrows) in the midline ventral to the neural tube. At later stages, signals (arrows) extended to the forebrain (fb), hindbrain (hb), and trunk regions of NC and NC derivatives. Signals were not obvious in the midbrain (mb) region. Cre negative control littermates (a, bottom; b–g, right) were devoid of β-gal signal. Scale bars: 500 μm

recombined allele was reliably detected at E9.5 (Figure 1f, E9.5, lane 5–7). These data suggest that Cre-dependent DNA recombination is inconsistent in *CAAG-lacZ* early stage (≤E8.5) embryos.

3.2 | *P0-Cre/R26-lacZ* labels NC cells and derivatives in early embryos

P0-Cre/CAAG-lacZ has been reported to label NC cells and derivatives after E9.0 (Yamauchi et al., 1999). Because the *R26-lacZ* reporter is more accessible to Cre-mediated DNA recombination than the *CAAG-lacZ* described above, we used the *R26-lacZ* reporter to re-examine *P0-Cre* transgene activity in early embryos at different somite stages using X-gal staining in whole embryo tissue.

At the 4-somite stage (E8.5), signals emerged in the midline of the neural groove region (Figure 2a,a', arrows). In the 6-somite embryo

(E8.5) (Figure 2b,b'), β-gal positive signals were found in the forebrain, hindbrain (arrows, Figure 2b'), first branchial arch and midline of the trunk neural groove region (Figure 2b,b'). The staining pattern in the 9-somite embryo was similar to that of the 6-somite stage but extended more caudally and β-gal signals were obvious in the midline and otic placodes (arrows, Figure 2c,c'). At the 12-somite (Figure 2d,d'), intense staining was found in the hindbrain region, branchial arches, otic placodes (arrows, Figure 2d'), and optic eminences. In the trunk region, signals were apparent in the neural groove area and in lateral tissues (Figure 2d,d'). At the 17-somite stage, positive signals were extensively distributed in the embryo, adding more labeled tissue regions that included the heart, frontonasal, and eye regions (Figure 2e). At the 22–26 somite stages, β-gal positive signals were extensively distributed in NC derivatives throughout the body, for example, frontonasal and eye regions, branchial arches, heart, and dorsal root ganglia (Figure 2f,g).

Notably, signals in the midbrain region were not apparent throughout the examined stages (Figure 2a–g). In littermate control embryos, no positive signals were observed within the embryos at the stages examined (Figure 2a–g).

3.3 | *P0-Cre* transgene expression is restricted to migrating NC cells and notochord in early embryos

To analyze *P0-Cre* expression in cranial NC, we used a monoclonal antibody against Cre to examine Cre immunoreactivity at different early somite stages of embryos. Specificity of Cre immunosignals were validated by three different methods: (1) Western blotting analysis to demonstrate the presence of a single band of expected size in a genotype-dependent manner (Supporting Information Figure 1), (2) immunohistochemistry using Cre$^-$ embryos labeled with primary antibody to show no signals (Supporting Information Figure 2), and (3) immunohistochemistry using Cre$^+$ embryos without the primary antibody to determine background levels (Figures 3 and 4).

β-gal signals in the *P0-Cre/R26-lacZ* embryo emerged in the neural groove region during the 4-somite stage (Figure 2a). We further identified the location and types of cells that express *P0-Cre* transgene through investigating immunoreactivity for Cre recombinase and colocalization with a NC cell marker SOX9 (Figure 3a,b) and a notochord marker FOXA2 (Figure 3c) in serial sections of 4-somite embryos ($n = 7$). Cre$^+$ signals were seen in a cluster of cells ventrally adjacent to the neural groove at the midbrain (Figure 3a, white arrowheads) and hindbrain levels (Figure 3b,c, white arrowheads), which is consistent with the *P0-Cre/R26-lacZ* whole mount staining for the reporter activity (Figure 2a). Cre immunosignals in clustered cells in the midline and ventrally adjacent to floor plate colocalized with SOX9 (arrowheads, Figure 3a,b) and FOXA2 (arrowheads, Figure 3c). However, Cre immunosignals were not detected in SOX9$^+$ cells in the neural plate border or mesoderm layer (arrows, Figure 3a,b) nor in the FOXA2$^+$ cells seen in the floor plate (arrows, Figure 3c). Nonspecific immunosignals from the secondary antibody were seen in the foregut diverticulum (dashed outlines, Figure 3b,c), which were confirmed by staining while omitting primary antibody (dashed outlines, Figure 3d).

At the 7–8 somite stage ($n = 3$), another NC marker p75$^+$ or/and SOX9$^+$ cells were seen at all brain levels examined, that is, forebrain, midbrain (Figure 4a), and hindbrain (Figure 4b). No Cre immunosignals were seen in the midbrain (Figure 4a). In the hindbrain region Cre immunosignals were detected in a small population of p75$^+$SOX9$^+$ cells in the mesodermal layer (arrows, Figure 4b), and in the mesenchyme of prospective branchial arch 1 (white arrowheads, Figure 4b). Cre immunoreactivity was also apparent in FOXA2$^+$ cells in the notochord region, that is, clustered cells ventrally adjacent to the floor plate (white arrowheads, Figure 4d) but not in the FOXA2$^+$ cells seen in the floor plate (arrows, Figure 4d). Again, nonspecific signals were seen in the foregut diverticulum when using secondary antibody for Cre immunoreactions, which was confirmed by staining while omitting primary antibody (white dashed outlines, Figure 4b,d,e).

In 14-somite embryos ($n = 3$), Cre$^+$ cells were abundantly distributed in the forebrain region and the immunosignals colocalized with SOX9 and

p75 (Figure 5a, arrowheads). Additionally, Cre signals were seen in some of the SOX9$^+$p75$^+$ cells in the anterior hindbrain region (Figure 5a, arrows). At the posterior hindbrain level (Figure 5b), an increasing intensity gradient of Cre immunoreactivity was observed from the dorsal to ventral region, that is, no immunosignals in the dorsal most part, faint immunosignals in the trigeminal NC region (Figure 5b, tn), obvious immunosignals in the branchial arch 1 region (Figure 5b, ba1), and intense immunosignals in the optic eminence (Figure 5b, oe). Similarly, the proportions of Cre$^+$SOX9$^+$p75$^+$ cells relative to total SOX9$^+$ or/and p75$^+$ cells in different regions were different. In the dorsal most part, some SOX9$^+$ cells in the neural fold region, presumably pre-migratory NC cells, were observed and negative for Cre immunoreactivity (open arrowheads, Figure 5c). In the trigeminal NC region, a subpopulation of SOX9$^+$p75$^+$ cells was Cre$^+$ (white arrows, Figure 5c). In the primordium of branchial arch 1, Cre immunosignals were apparent in a significant population of SOX9$^+$p75$^+$ cells (arrows, Figure 5d). In the optic eminence most, if not all, SOX9$^+$p75$^+$ cells were brightly labeled with Cre (white arrows, Figure 5e). Importantly, Cre$^+$ cells were not seen in the Sox9$^-$ and p75$^-$ cells in any tissue regions. In the negative control slides (Cre$^-$ embryo sections with primary antibody staining and Cre$^+$ embryo sections without primary antibody), no immunosignals were seen in the 14-somite embryo tissue (Supporting Information Figure 2).

Compared to the 14-somite stage, 19-somite embryos ($n = 4$) had a similar distribution pattern of Cre immunosignals, that is, an increasing intensity gradient from the dorsal to ventral regions of the tissue (Figure 6a,b). Additionally, increasing proportions of Cre$^+$SOX9$^+$ cells relative to the total number of SOX9$^+$ cells were observed from dorsal to ventral regions (Figure 6c–e). However, the proportions of Cre$^+$SOX9$^+$ cells relative to total SOX9$^+$ cells in all regions were lower than those at the 14-somite stage. At the anterior hindbrain level, Cre$^+$ immunosignals were seen in some of the SOX9$^+$ cells in the hindbrain and intense signals were distributed in the majority of SOX9$^+$ cells in the forebrain (Figure 6a, arrows). At the posterior hindbrain level, Cre$^+$ cells were seen in the trigeminal NC (Figure 6b,c, tn), branchial arch 1 (Figure 6b,d, ba1), and optic eminence (Figure 6b,e, oe). The intensity of Cre immunosignals in the optic eminence was diverse in the SOX9$^+$ cells, some of which were negative for Cre (arrowheads, Figure 6e), which is in contrast to almost all of SOX9$^+$ cells that showed presence of Cre immunosignals in the 14-somite embryos (Figure 5e).

3.4 | *P0-Cre* labeled cells are distributed in cranial NC and derivatives in early embryos and newborn mice

To confirm the specific labeling of *P0-Cre/R26-lacZ* and Cre immunosignals, we used another *Cre* reporter line (*R26-RFP*) and found that the distribution pattern of *P0-Cre/R26-RFP* signals (11s, Figure 7) was the same as *P0-Cre/R26-lacZ* (Figure 2d, d'), that is, signals were found in the hindbrain region, branchial arches, in the neural groove area and lateral tissues in the trunk region (Figure 7a). Similar to *lacZ* expression in *P0-Cre/R26-lacZ* embryos, RFP signals were not apparent in the midbrain region (mb). On tissue sections at the posterior hindbrain level, Cre immunosignals and RFP signals largely colocalized (Figure 7b). Again, an increasing gradient of Cre and RFP signal intensity and
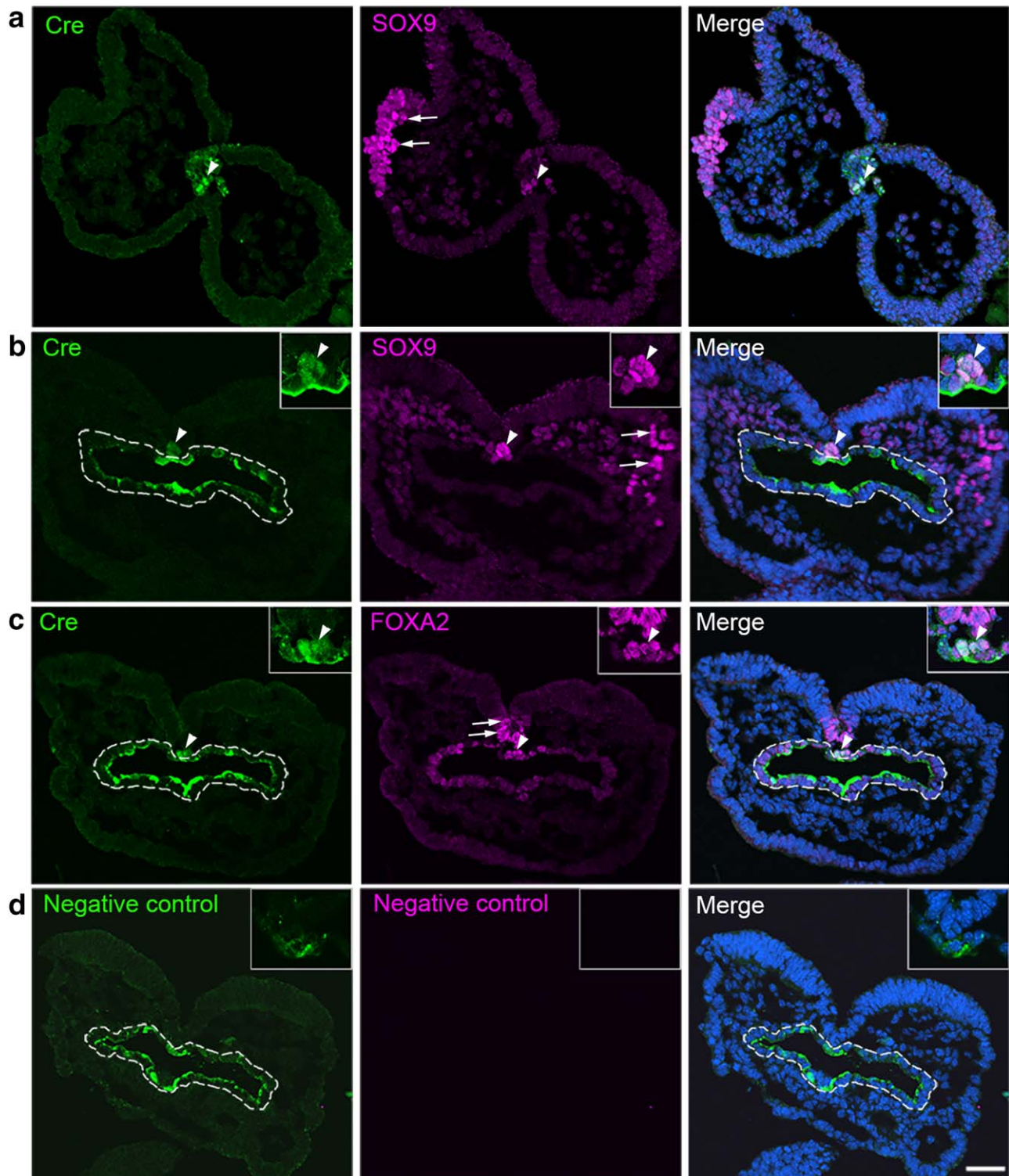
FIGURE 3 Single-plane laser scanning confocal photomicrographs of transverse sections of a 4-somite *P0-Cre* embryo. Sections were immunostained using an antibody against Cre (green) and were double labeled with SOX9 (purple, a,b) or FOXA2 (purple, c). Arrowheads point to Cre immunoreactive cells co-labeled with SOX9 (a,b) or FOXA2 (c) in the notochord region. Arrows point to single labeled SOX9$^+$ cells in the NC cell region (a,b) and FOXA2$^+$ cells in the floor plate of neural tube (c). White dashed lines outline the foregut diverticulum (b–d). In the negative control slide (d), primary antibodies were omitted. Scale bar: 50 μm for all images

proportions of labeled cells was observed from the dorsal to ventral region, that is, no signals in the dorsal-most part, faintly labeled cells were sparsely found in the trigeminal NC region (Figure 7b, tn), obvi-ously and frequent labeled cells (Cre$^+$RFP$^+$) in the branchial arch 1 region (Figure 7b, ba1), and intensely and mostly labeled in the optic eminence (Figure 7b, oe). Auto-fluorescent blood cells and noncellular
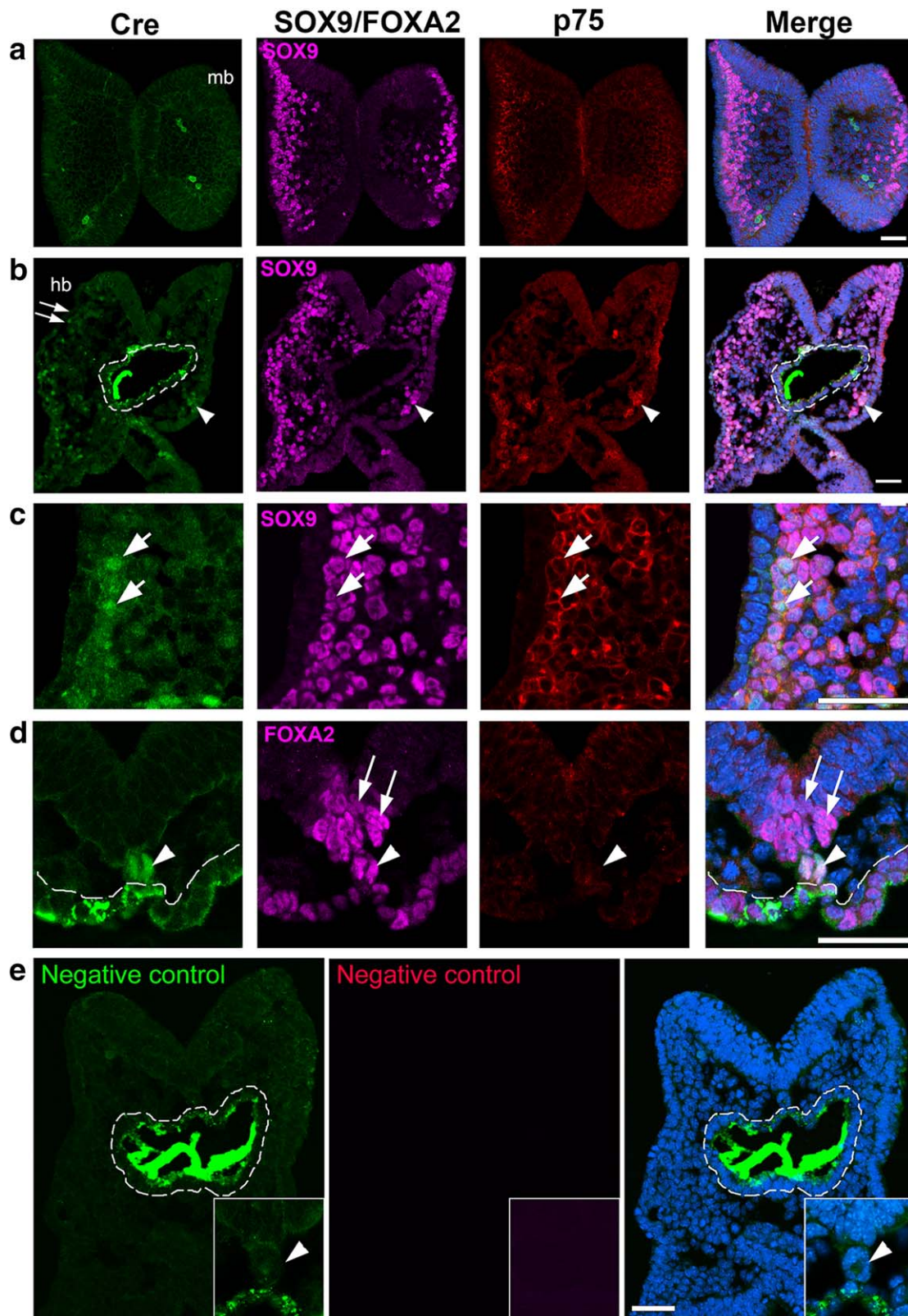
FIGURE 4 Immunoreactivity of Cre (green, a–d), SOX9 (purple, a–c) or FOXA2 (purple, d), and p75 (red, a–d) in transverse sections of a 7-somite *P0-Cre* embryo at the midbrain (a) and hindbrain-forebrain (b–e) levels. Arrows in (c) point to some of the triple labeled Cre$^+$SOX9$^+$p75$^+$ cells in the NC cell region. Arrowheads in (d) point to Cre$^+$ cells colabeled with FOXA2 in the notochord region and arrows to FOXA2$^+$ cells in the floor plate of neural tube (d). White dashed lines outline the foregut diverticulum (b, d, and e). In the negative control slide (e), primary antibodies were omitted and only secondary antibodies were applied. Scale bar: 50 μm for all images (single-plane laser scanning confocal)
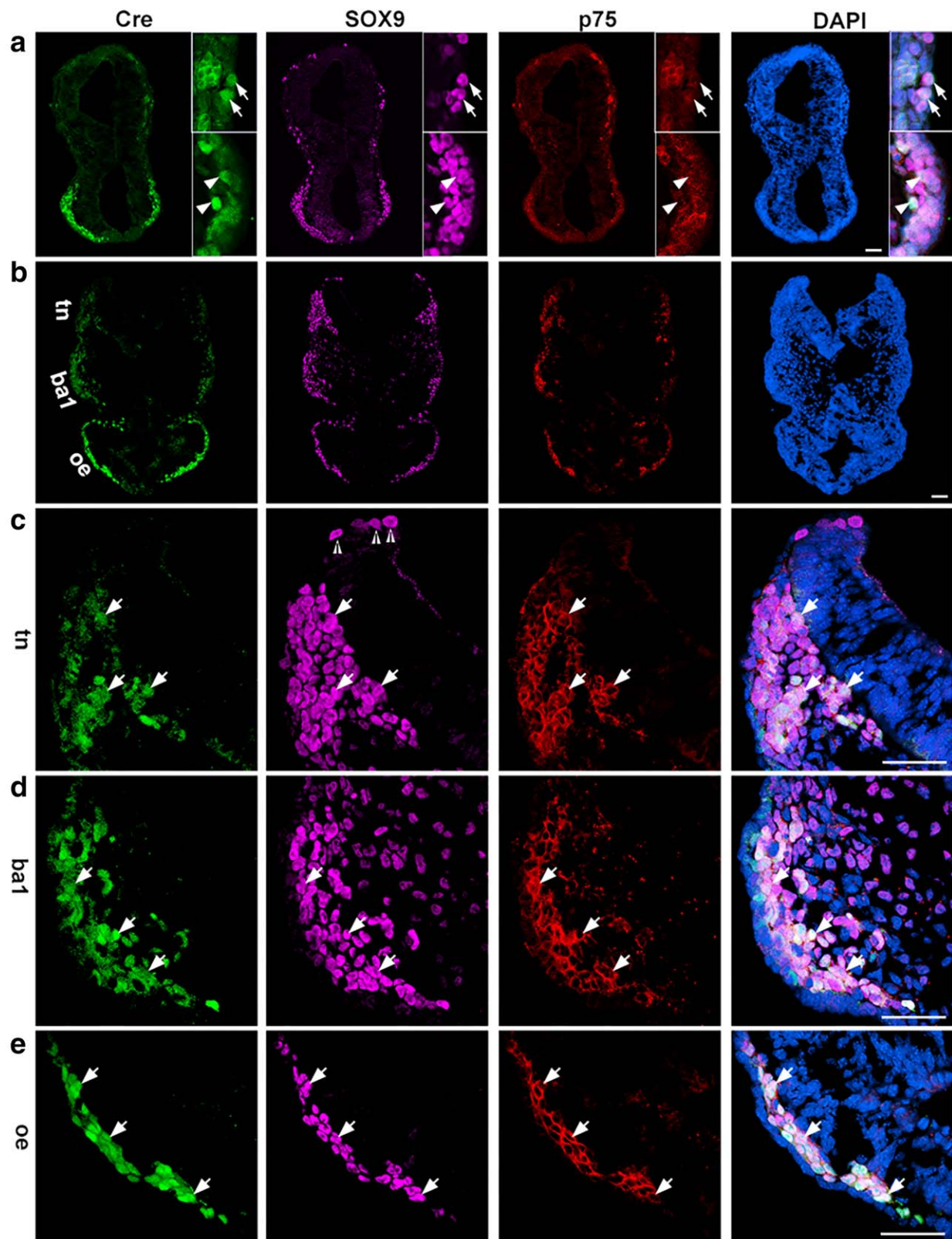
FIGURE 5 Photomicrographs of transverse sections of a *P0-Cre* embryo at the 14-somite stage. Sections were immunostained for Cre (green), SOX9 (purple), and p75 (red) at the anterior hindbrain-forebrain level (a) and posterior hindbrain-forebrain level (b). (c–d) are higher magnification images of trigeminal NC (c, tn), branchial arch 1 (d, ba1), and optic eminence (d, oe). Arrows (a) point to Cre$^+$ cells that were colabeled with SOX9 and p75 immunosignals in the anterior hindbrain regions, and arrowheads (a) point to triple labeled Cre$^+$SOX9$^+$p75$^+$ cells in the forebrain regions. Open arrowheads (c) point to SOX9$^+$ cells in the neural fold region, presumably premigratory NC cells. Arrows (c–e) point to Cre$^+$ cells colabeled with SOX9$^+$ and p75$^+$, presumably migratory NC, in trigeminal NC regions (tn, c), first branchial arch 1 (ba1, d) and optic eminence (oe, e). Scale bars: 50 μm for all images (single-plane laser scanning confocal)
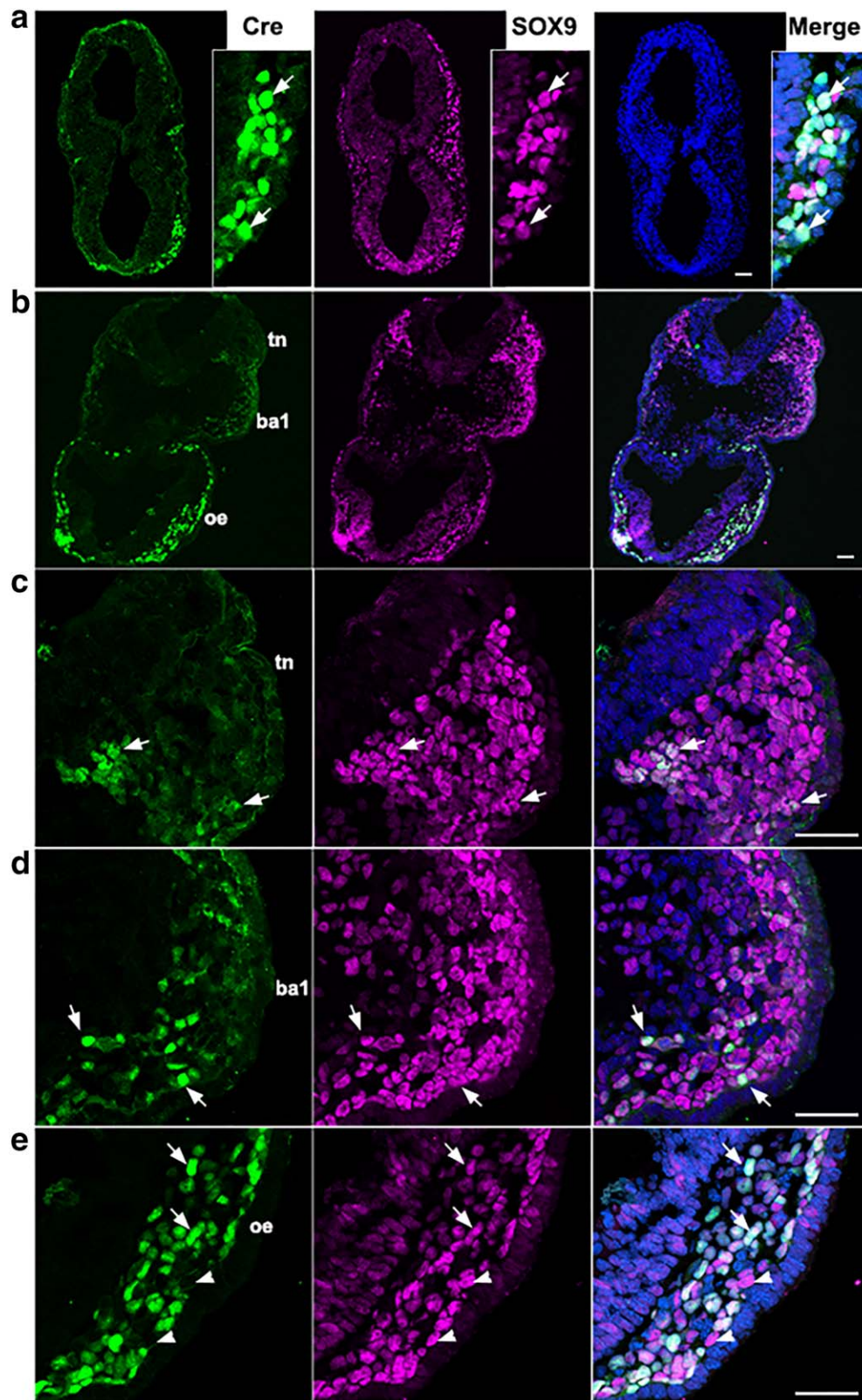
FIGURE 6 Single-plane laser scanning confocal photomicrographs in transverse sections of a 19-somite *P0-Cre* embryo. Sections were immunostained using an antibody against Cre (green) and were double labeled with SOX9 (purple, a–e). (c–d) are higher magnification images of trigeminal NC (c, tn), branchial arch 1 (d, ba1), and optic eminence (d, oe). Arrows (a) point to Cre$^+$ cells that were co-labeled with SOX9 in the forebrain. Arrows (c–e) point to Cre$^+$ cells co-labeled with SOX9 in trigeminal NC regions (tn, c), branchial arch 1 (ba1, d), and optic eminence (oe, e). Arrowheads in e point to SOX9$^+$ cells without Cre immunosignals. Scale bars: 50 μm, also applies to other images in the same panel
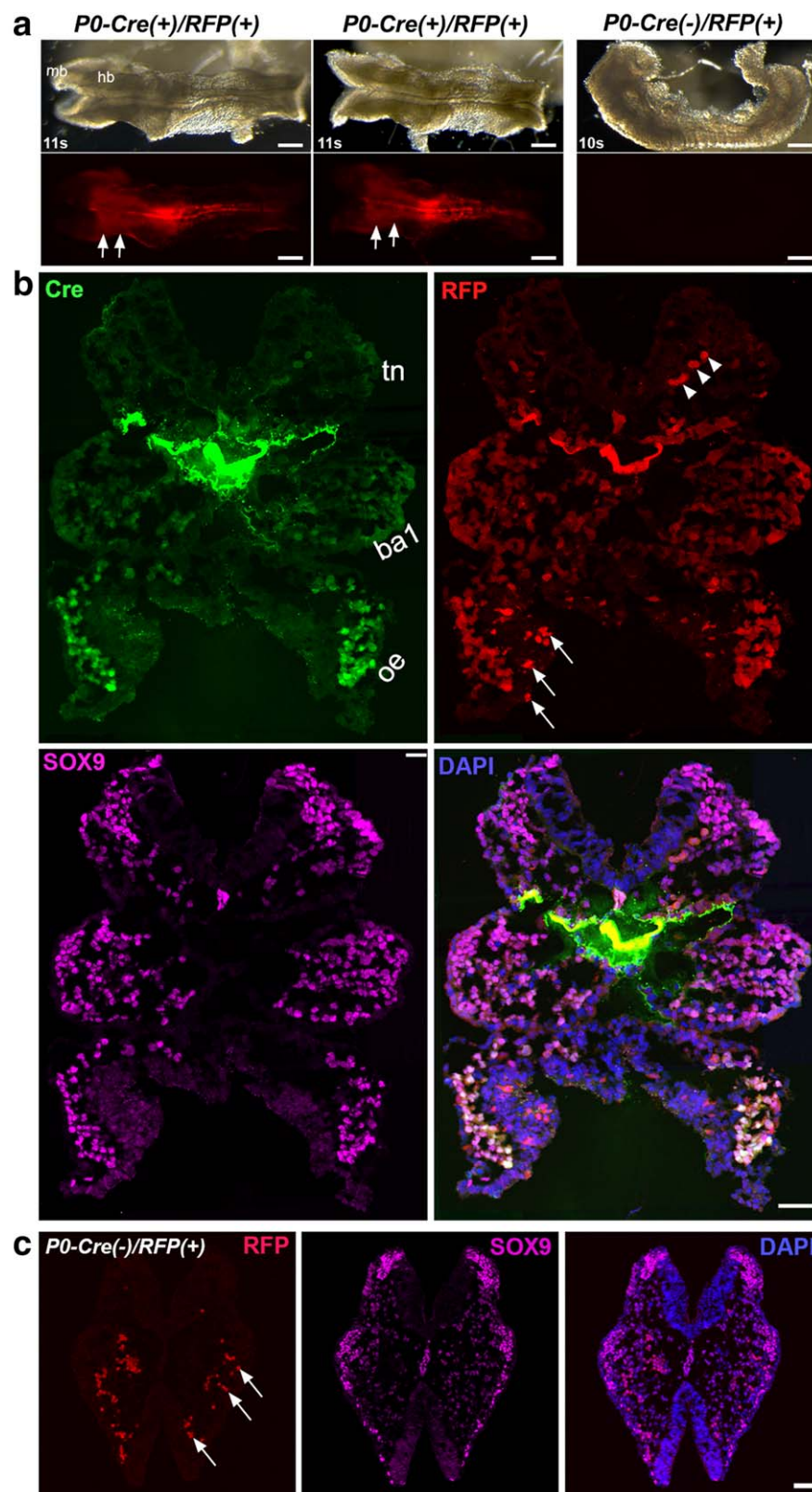
FIGURE 7 Consistent distribution of Cre and RFP signals in *P0-Cre/R26-RFP* embryos with that in *P0-Cre* and *P0-Cre/R26-lacZ* embryos. (a): Bright-field (top panel) and fluorescent (bottom panel) images of whole *P0-Cre/R26-RFP* embryos at 10–11 somite stages. The midbrain (mb) region was devoid of RFP signals. Arrows point to the hindbrain region labeled with RFP. (b): Single-plane laser scanning confocal photomicrographs of a transverse section of an 11-somite *P0-Cre(+)/R26-RFP(+)* embryo at the hindbrain level. An increasing intensity gradient of Cre and RFP signals from the dorsal to ventral region, that is, faint and sparse in the trigeminal NC (tn), clear and frequent in the branchial arch 1 (ba1), bright and almost all in the optic eminence (oe). Arrowheads point to the autofluorescent blood cells. Arrows point to some noncellular RFP+ fragments. (c): Confocal images of a transverse section of a 10-somite Cre− embryo to illustrate the autofluorescent blood cells and non-cellular RFP+ fragments (arrows). Scale bars: 200 μm in (a); 50 μm in (b and c)
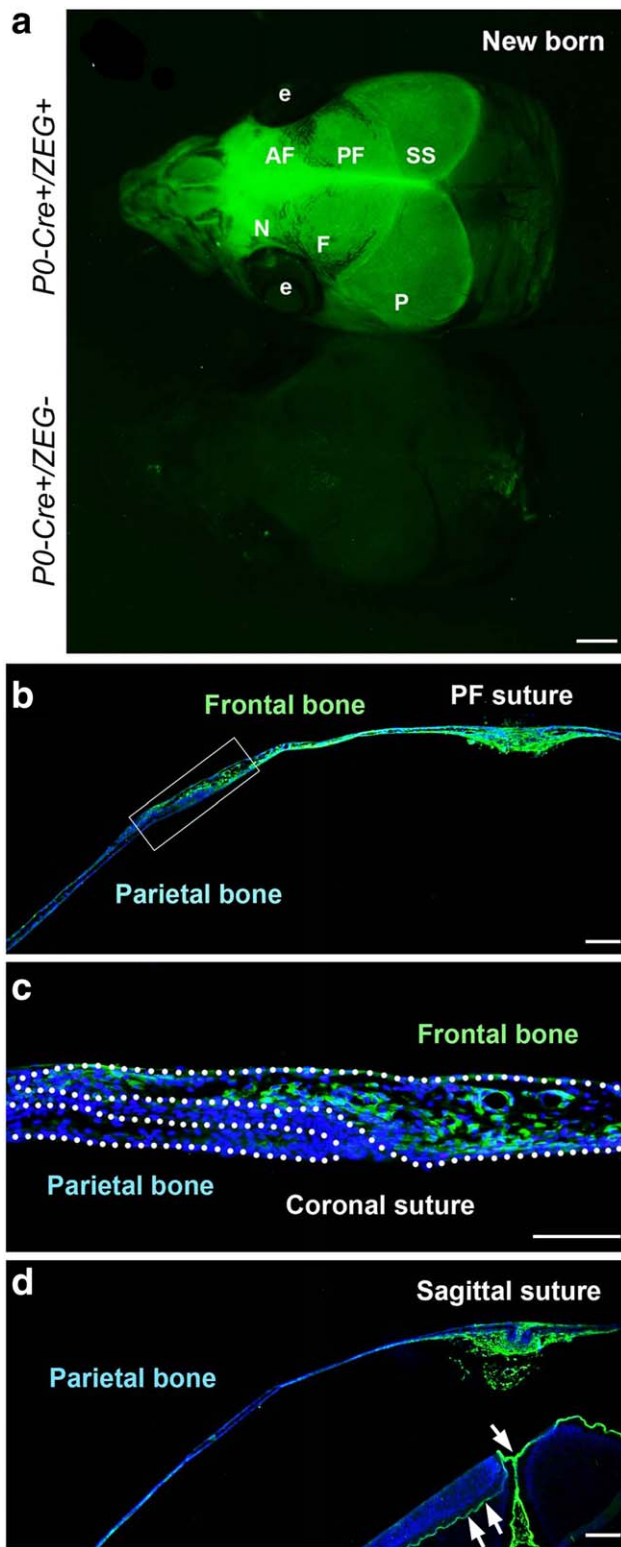
FIGURE 8 *P0-Cre* marks cranial NC and derived cells in the skull. (a): GFP signals in the newborn *P0-Cre*[+]/*ZEG*[+] (upper) and control littermate (bottom) mice. (b): GFP signals on the coronal tissue sections illustrate that the frontal bones (b,c), but not the parietal bone (c,d), were labeled. (c) is the high magnification image of the squared tissue region in (b). Abbreviations: AF, anterior frontal suture; e, eye; F, frontal bone; N, nasal bone; P, parietal bone; PF, posterior frontal suture; SS, sagittal suture. Scale bars: 500 μm in (a), 200 μm in (b) and (d); 100 μm in (c)

RFP[+] fragments were also seen (Figure 7b, arrowheads) and confirmed in the Cre[−] tissue sections (Figure 7c, arrowheads).

To verify the specificity of *P0-Cre* in labeling NC cells and derivatives, we examined whether *P0-Cre* faithfully labels the nasal and frontal bones in the skull that are well-characterized cranial NC derivatives. Consistent with a previous report using *Wnt1-Cre* mice (Jiang et al., 2002), *P0-Cre* successfully labeled both nasal and frontal bones along with dura mater (Figure 8a–c). Importantly, *P0-Cre* did not label the parietal bones that are known as paraxial mesoderm derivatives (Figure 8c,d) (Chai and Maxson, 2006; Noden and Trainor, 2005). The fluorescent signals in the parietal bone region of whole mount tissue (Figure 8a) were confirmed on sections to be from the underlying meninges (arrows, Figure 8d), which are NC derivatives (Jiang et al., 2002).

3.5 | Different distribution pattern of *Wnt1-Cre* labeling from *P0-Cre* in cranial regions

In *P0-Cre/R26-lacZ* embryos (Figure 2), reporter labeling was not apparent in the midbrain region. To further examine our observation, *R26-lacZ* was crossed with *Wnt1-Cre*, which is well known for labeling midbrain.

At the 6-somite stage (Figure 9a), the signals in *Wnt1-Cre/R26-lacZ* mouse embryos were intense in the midbrain and along the midline of the neural groove (Figure 9a). In the 8-somite embryo (Figure 9b), β-gal positive signals were extensively distributed in the midbrain (Figure 8b). However, signals in the hindbrain were absent at the 6-somite stage (Figure 9b, arrows) and were sparse at the 8-somite stage (Figure 9b, arrows). At E10.5, the signals extended to the forebrain (fb), midbrain (mb), hindbrain (hb) and trunk regions of NC and NC derivatives in *Wnt1-Cre/R26-lacZ* embryos (Figure 9c), for example, frontonasal and eye regions, branchial arches, heart, and dorsal root ganglia. In contrast to the extensive labeling of *Wnt1-Cre* in the midbrain, *P0-Cre* labeling in midbrain was not obvious (Figure 9c), which is consistent with our earlier observations (Figure 2).

Next, we further analyzed the expression patterns of *Wnt1-Cre* transgene in cranial NC using the antibody for Cre recombinase. In the 4-somite embryos (Figure 10a), Cre immunosignals were found in SOX9^{+} pre- and post-migratory NC cells and in the neural epithelium at the midbrain level (Figure 10a). In contrast, SOX9^{+} migrating NC cells were negative for Cre in the hindbrain region (arrows, Figure 10b). At the 7-somite stage (Figure 10c), Cre immunosignals were extensively distributed in migrating NC cells in the midbrain and forebrain regions, in addition to labeling of part of the neuroepithelium. Again, in hindbrain regions, Cre immunosignals were observed only in the neural fold and were not apparent in SOX9^{+} migrating NC cells (arrows, Figure 10d). This is an interesting contrast to the abundant Cre immunosignals found in the hindbrain region of *P0-Cre* embryos at the 7-somite stage (arrows, Figure 4b,c). At the presumptive notochord regions, no Cre immunosignals were seen in *Wnt1-Cre* embryos (arrowheads, Figure 10b,d). In the 16-somite embryos, Cre immunosignals were found in the midbrain and forebrain but were not apparent in the hindbrain (Figure 10e), which is in contrast to the distribution of Cre immunosignals in the 16–19 somite *P0-Cre* embryos (Figures 5 and 6).
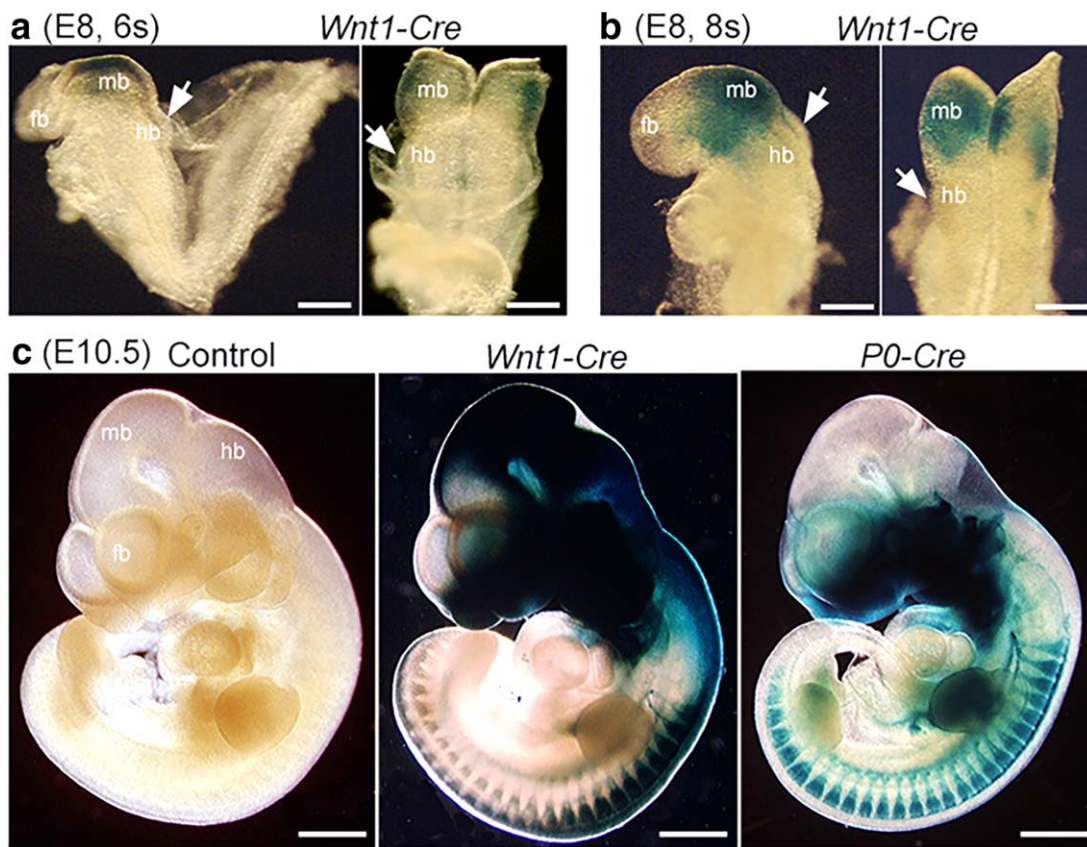
FIGURE 9 Whole mount X-Gal visualization of *lacZ* gene product β-galactosidase in *Wnt1-Cre/R26-lacZ* mouse embryos at different stages (E8-E10.5). β-gal positive signals (blue) were extensive in the midbrain (mb) at the 6s (a) and 8s (b) stages, but were sparse in the hindbrain. At later stages, signals extended to the forebrain (fb), midbrain (mb), hindbrain (hb) and trunk regions of NC and NC derivatives in *Wnt1-Cre/R26-lacZ* tissue at E10.5 (c). In E9 *P0-Cre/R26-lacZ* mouse embryos (c), β-gal positive signals (blue) were found in the forebrain (fb), hindbrain (hb) and trunk regions of NC and NC derivatives, but were not apparent in the midbrain (mb). Scar bars: 200 μm in (a and b); 1 mm in (c)

In the trigeminal NC regions (tn), first branchial arch 1 (ba1) and optic eminence region (oe), Cre immunosignals were sparsely seen in migratory NC cells (Figure 10f).

Also, *R26-RFP* Cre reporter was used to confirm the specific labeling of *Wnt1-Cre* driven *R26-lacZ* and Cre immunoreactivity. The distribution pattern of signals in *Wnt1-Cre/R26-RFP* embryos (Figure 11a, 5–7s) was identical to that of *Wnt1-Cre/R26-lacZ* embryos (Figure 9a,b, 6–8s). The signals in *Wnt1-Cre/R26-RFP* mouse embryos were intense in the midbrain (Figure 11a, arrowheads), and signals in the hindbrain were not obvious at the 6- and 7-somite stages (Figure 11a, arrows). On tissue sections of a 6-somite *Wnt1-Cre/RFP* embryo, the distribution of RFP$^+$ cells was coincident with that of Cre$^+$ cells (Figure 11b,c), such as abundance within migrating NC cells in the midbrain and in the forebrain neuroepithelium (Figure 11b). The labeling was sparse among migrating NC cells in the hindbrain region (arrows, Figure 11c).

Taken together (Table 1 and Supporting Information Figure 3), both *P0-Cre* and *Wnt1-Cre* label cranial NC cells, peaked at 7-somite stage in *Wnt1-Cre* and 14-somite in *P0-Cre*. An overlap (in forebrain) but distinct (*Wnt1-Cre* in midbrain and *P0-Cre* in hindbrain) distribution patterns of the Cre activities were observed. In addition to NC, both

P0-Cre and *Wnt1-Cre* labeled other cells, for example, notochord was labeled by *P0-Cre* and neuroepithelium by *Wnt1-Cre*.

4 | DISCUSSION

The *P0-Cre* transgenic mouse line has been widely used for NC cell fate mapping (Feltri et al., 1999b; Ono et al., 2015; Sommer and Suter, 1998) and genetic modifications of NC-derived cells (Hu, Strobl-Mazzulla, & Bronner, 2014; Liu and Xiao, 2011). However, questions remain about how early, how specifically, and to what extent *P0-Cre* transgene labels NC cells in early embryos. Moreover, concerns about the specificity of *P0-Cre* and other Cre models in labeling NC lineage have been raised (Trainor, 2005a,b). Therefore, a detailed analysis of *P0-Cre* transgene activity is essential for the use and data interpretation of this model. In the present study, we found that the *CAAG-CAT-Z* (*CAAG-lacZ*) Cre reporter mice used in the original report (Yamauchi et al., 1999) did not appropriately reflect Cre activity in early stage embryos. We then investigated Cre activity using a *R26-lacZ* reporter and Cre immunoreactivity to find *P0-*
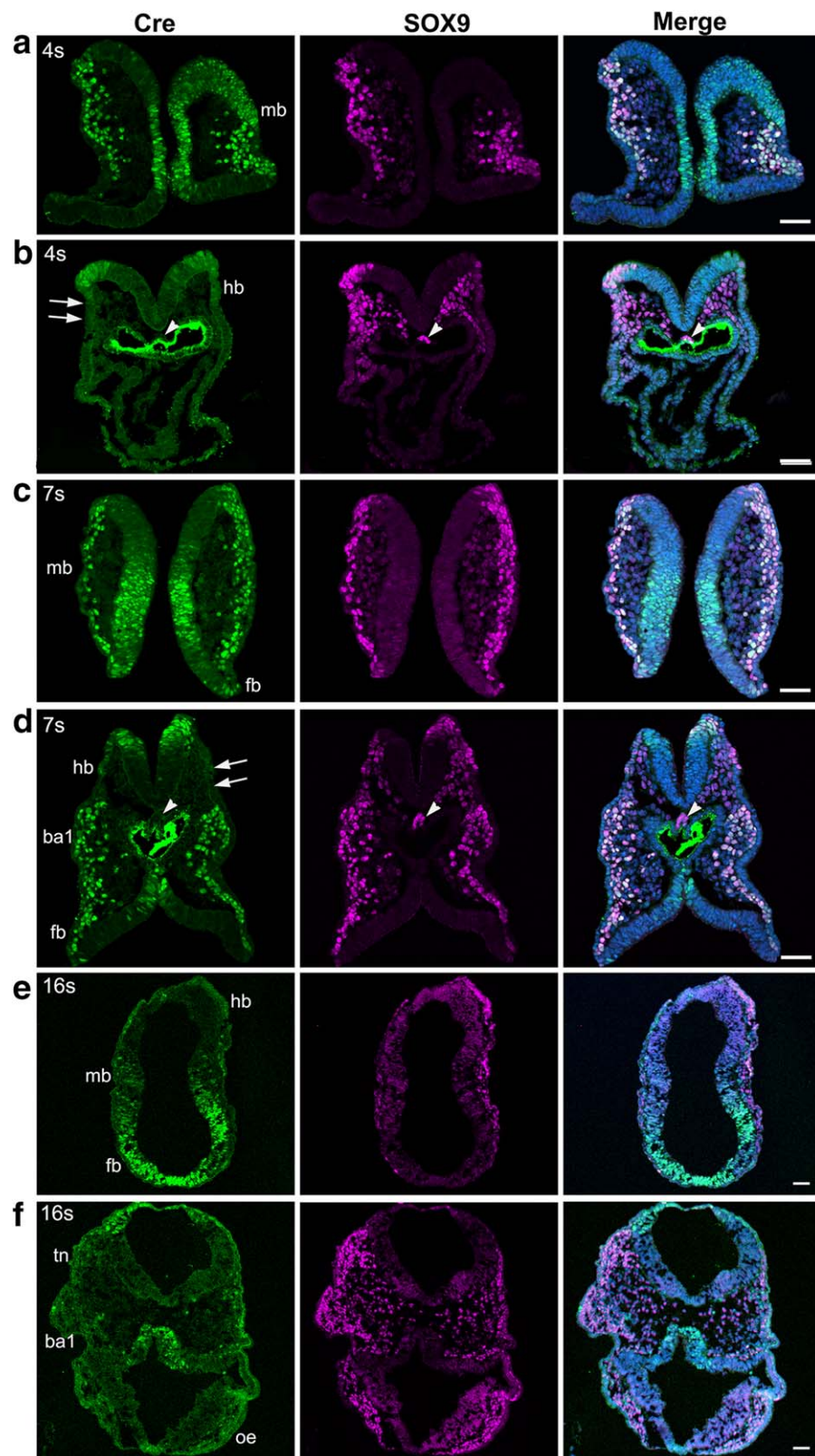
FIGURE 10 Photomicrographs from sections of E8.5 *Wnt1-Cre* embryos at different somite stages immunostained for the Cre and NC cell marker SOX9. At the 4–7 somite stages (a–d), Cre immunosignals (green) were bright in the midbrain (a, c) and derived NC cells and colocalized with SOX9 (purple). In contrast, in the hindbrain-forebrain levels (b, d) Cre immunosignals were seen in SOX9$^+$ premigratory NC cells but were absent in migrating NC cells. In 16-somite embryos (e, f), Cre immunosignals were seen in migrating NC cells in the midbrain and forebrain regions (e). In the trigeminal NC regions (tn), first branchial arch 1 (ba1), and optic eminence region (oe), Cre immunosignals were sparse in migratory NC cells. Scale bars: 50 μm (single-plane laser scanning confocal)
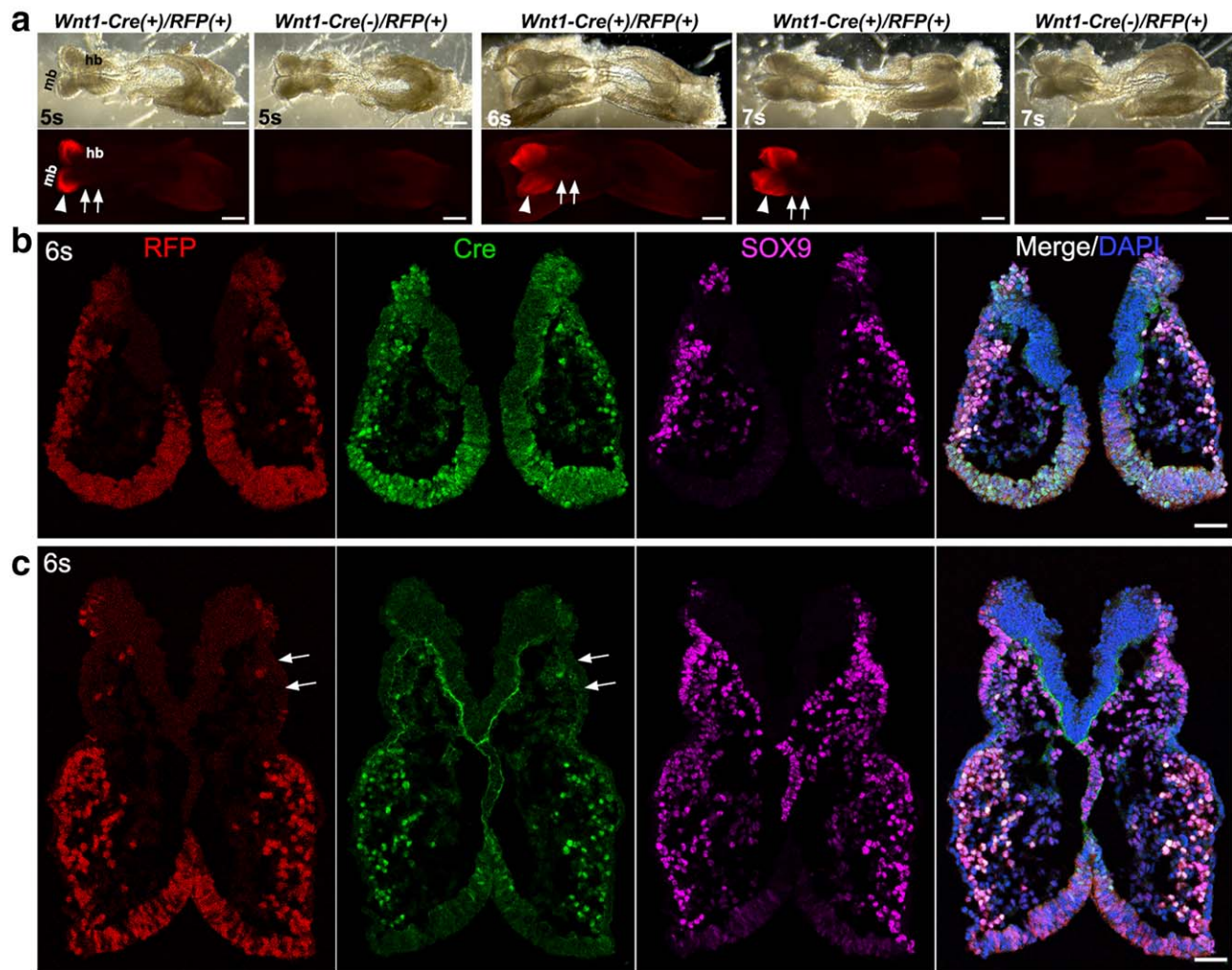
FIGURE 11 Distribution of Cre and RFP signals in *Wnt1-Cre/R26-RFP* embryos. (a): Bright-field (top panel) and fluorescent (bottom panel) images of whole *Wnt1-Cre/R26-RFP* embryos at 5–7 somite stages. In contrast to the *P0-Cre/R26-RFP* embryos, RFP signals were detected in midbrain (mb) region (arrowheads), but not obvious in the hindbrain (hb, arrows). (b and c): Single-plane laser scanning confocal photomicrographs of a transverse section of a 6-somite *Wnt1-Cre(+)/R26-RFP(+)* embryo at the midbrain (b) and hindbrain (c) level. Arrows (c) point to the trigeminal NC region that was devoid of RFP and Cre signals. Scale bars: 250 μm in (a); 50 μm in (b) and (c)

Cre expression as early as the 4-somite stage in notochord labeled with FOXA2 and in the migrating NC cells at the 7-somite stage using the commonly used NC cell markers SOX9 (Mori-Akiyama, Akiyama, Rowitch, & de Crombrugghe, 2003; Sahar, Longaker, & Quarto, 2005; Spokony et al., 2002) and p75 (Young, 2000; Young, Ciampoli, Hsuan, & Canty, 1999). Cre immunosignals were especially extensive in the forebrain and hindbrain but not apparent in the midbrain. Importantly, Cre immunosignals were not seen outside of the NC cell population and notochord. Given the fact that notochord derivatives are well-known to be restricted to the intervertebral disc (McCann, Tamplin, Rossant, & Seguin, 2012; Yamauchi et al., 1999), our data demonstrated that *P0-Cre* can serve as a valuable tool for studies on NC cell lineage, especially for forebrain and hindbrain NC derivatives. In contrast, *Wnt1-Cre* extensively labeled pre- and post-migratory NC cells at the midbrain level, but only sparsely in the trigeminal NC region at the hindbrain level. Additionally, *Wnt1-Cre* labeled a large population of non-NC cells in the neu-

ral plate, which is consistent with previous reports (Echelard et al., 1994; Rowitch et al., 1998).

4.1 | *P0-Cre* specifically labels a significant population of, if not all, migrating NC cells and notochord

The specificity of Cre expression in the NC cell population was examined with two commonly used NC cell markers, p75 (Menendez, Yatskievych, Antin, & Dalton, 2011) to label migrating NC and SOX9 (Nakanishi, Chan, & Ito, 2007; Pomp, Brokhman, Ben-Dor, Reubinoff, & Goldstein, 2005) to label both pre- and post-migratory NC cells. Our data support the idea that *P0-Cre* specifically labels migrating NC cells and notochord based on the following observations: (1) Cre immunosignals were only detected in $p75^+SOX9^+$ double labeled cells, and were more intense in the NC cells that were close to their destinations; (2) importantly, Cre immunosignals were not seen outside of the $p75^+SOX9^+$ double labeled cells; (3) Cre immunosignals were not seen

TABLE 1 Comparison between *P0-Cre* and *Wnt1-Cre* in labeling cranial neural crest (NC), neural epithelium (NE), and notochord to various extent

Cranial regions		*P0-Cre*	*Wnt1-Cre*
Forebrain	NC	++	++
	NE	−	++
Midbrain	NC	−	++
	NE	−	+
Hindbrain	NC	++	±
	NE	−	±
Notochord		+	−

++ extensively; + clearly; ± rarely; − negatively.

in SOX9$^+$ cells in the neural fold region, which presumably premigratory NC cells, and Cre immunosignals were rarely detectable in the immediately delaminated NC cell region; and (4) Cre immunosignals only colocalized with FOXA2 in the notochord region, and were absent in FOXA2$^+$ cells in the floor plate. These data demonstrate that *P0-Cre* is specific in labeling migrating NC cells and notochord. An increasing gradient of intensity of Cre immunosignals and RFP signals was observed from the dorsal to ventral regions suggesting that the expression of *P0-Cre* transgene in the NC cells is obtained during migration. Our data are valuable in demonstrating the specificity of *P0-Cre* in labeling NC cells in early embryos. The specificity of *P0-Cre* in labeling cranial NC cells was further confirmed by the distribution of *P0-Cre* labeled cells in the well-known NC derivatives in the skull, for example, frontal bones and sutures, in contrast to the absence of labeled cells in the parietal bone that is known to be non-NC derived.

The notochord is a rod-shaped structure in the midline that is ventrally adjacent to the neural tube (Jurand, 1974). Studies using a *Cre* mouse line driven by the notochord-specific homeobox gene *Noto* that traced the cell fate of notochord demonstrated that notochord serves as a source of embryonic precursors of cells within the nucleus pulposus of the mature intervertebral disc (McCann et al., 2012). In our study, *P0-Cre* transgene expression was detected in the notochord region in the 4–7 somite stage embryos, which is consistent with a previous report demonstrating that *P0-Cre* transgene labels notochord in addition to NC cells and derivatives (Yamauchi et al., 1999). With exception to the labeling of notochord, *P0-Cre* labels migrating NC cells specifically. Indeed, our data using *P0-Cre* to mark cranial bones, that is, nasal and frontal but not parietal bone, further demonstrated the specificity of *P0-Cre* in labeling cranial NC derivatives and that *P0-Cre* mice can be considered as a useful tool to trace NC lineages, at least cranial NC-derived bones (Komatsu et al., 2013), during mouse embryonic development.

However, *P0-Cre* did not label all of the NC cells in all of the tissue regions. The proportions of Cre$^+$ cells relative to the total number of p75$^+$SOX9$^+$ cells were different in different tissue regions. NC cells migrate ventrally to their target tissue/organs and follow certain paths after delamination. Thus, the increasing intensity

gradient of Cre immunosignals and RFP signals and increasing cell proportions of Cre$^+$ and RFP$^+$ cells from dorsal to ventral regions suggest that *P0-Cre* transgene expression emerged during NC migration. Although Cre immunosignals were not detected in all the p75$^+$SOX9$^+$ cells, we cannot exclude the possibility that *P0-Cre* does indeed label all NC cells. It would be difficult to evaluate the exact proportion of *P0-Cre* transgene in labeling migrating NC cells because the expression is transient and because *P0-Cre* can be expressed in a NC cell for a short time frame at any time point. Our observation that detection of Cre immunosignals in all the p75$^+$SOX9$^+$ cells in the optic eminence and the majority of mesenchymal cells immediately under the epithelium of prospective branchial arch 1 at the 14 somite stage supports the idea that *P0-Cre* transgene is expressed in a significant population of, if not all, migrating NC cells in the forebrain and hindbrain regions.

Several Cre reporter lines have been generated and are widely used for cell fate mapping (Ikeya et al., 1997; Kawamoto et al., 2000; McMahon et al., 1992; Novak et al., 2000; Weissman and Pan, 2015; Weissman Sanes, Lichtman, & Livet, 2011). Among these reporter lines, *ROSA26* and *CAAG* are two commonly used promoters for driving reporter gene expression (Araki, Araki, Miyazaki, & Vassalli, 1995; Kawamoto et al., 2000). In the present study, the efficiency and reliability of two Cre reporters, *R26-lacZ* and *CAAG-lacZ*, were compared using *Mexo2-Cre*, in which Cre is expressed as early as E5.5 in epiblast (Tallquist and Soriano, 2000). We found that *R26-lacZ* reporter expression emerges earlier than *CAAG-lacZ* reporter expression and that DNA recombination in *R26-lacZ* was reliable and consistent with Cre expression. One interesting observation is that although all E9.5 *Meox2-Cre/CAAG-lacZ* embryos showed evidence of DNA recombination, the *lacZ* signals were weak, and were restricted to the heart and somites. It is possible that the promoter activity to drive *lacZ* expression in the *CAAG-lacZ* cassette was silenced or weaker than that of *R26-lacZ* in early stage embryos. Together, the data suggest that less efficient and inconsistent DNA recombination, and variable *CAAG* promotor activity might be the major reasons for this discrepancy.

4.2 | *P0-cre* labels cranial NC cells in a cranial region-specific manner

It has been reported that NC cells are generated by the 7-somite stage at all levels of the forebrain, midbrain, and hindbrain (Chan and Tam, 1988; Nichols, 1981; Serbedzija, Bronner-Fraser, & Fraser, 1992). By detecting both *R26-lacZ* reporter expression and Cre immunoreactivity we found that *P0-Cre* transgene expression emerges at the 7-somite stage in hindbrain and forebrain migratory NC cells. In the 14-somite embryos, we found strong Cre immunosignals in a considerable subpopulation of migrating NC cells labeled with SOX9 and p75 in the forebrain and hindbrain NC regions.

However, *P0-Cre* expression was rarely detected in the midbrain region, which is in contrast to extensive distribution of Cre immunosignals and RFP signals in the midbrain NC of *Wnt1-Cre* (Huang, Liu, Huang, Zhao, & Cheng, 2010; Lewis et al., 2013). At E8.5, when cranial NC cells emerge, *Wnt1-Cre* labels NC cells extensively in midbrain but

many fewer cells were seen in hindbrain (Danielian, Muccino, Rowitch, Michael, & McMahon, 1998; Echelard et al., 1994). *Wnt1* and *Wnt1-Cre* expression is not restricted to the NC domain but also labels dorsal neural stem cells that contribute to both the central nervous system and to neural progenitors (Barriga, Trainor, Bronner, & Mayor, 2015; McMahon et al., 1992). In the present study, we crossed the same *R26-lacZ* reporter mouse with *P0-Cre* and *Wnt1-Cre* and confirmed the labeling pattern (Figure 9). The difference between *P0-Cre* and *Wnt1-Cre* in labeling NC cells was profound in the midbrain and hindbrain, which may be why *P0-Cre* and *Wnt1-Cre* label different populations of cells in the orofacial organs, for example, tooth buds (Wang et al., 2011) and taste buds (Boggs et al., 2016; Liu et al., 2012).

It has been reported that forebrain crest cells appear by the 8–14 somite stages and migrate dorsally over the presumptive eye where they meet the ventrally migrating midbrain crest cells. Although we did not see much *Cre* reporter activity or Cre immunoreactivity in the midbrain, Cre immunoreactivity was detected in all the $SOX9^+p75^+$ cells in the optic eminence, which suggests that forebrain is the source of NC cells that contribute to optic eminence development.

5 | CONCLUSIONS

The *P0-Cre* transgenic mouse model was first generated to label NC derivatives (Yamauchi et al., 1999) and has been widely used for NC lineage tracing (Boggs et al., 2016; Kawakami et al., 2011; Liu et al., 2012; Ogawa et al., 2015; Wang et al., 2011) and genetic modification (Feltri et al., 1999a; Komatsu et al., 2013; Nomura-Kitabayashi et al., 2009; Ogawa et al., 2015). Differences have been found between *P0-Cre* and *Wnt1-Cre* in labeling NC lineage. Here, we re-visited the *P0-Cre* model at early embryonic stages and demonstrated that *P0-Cre* transgene specifically labels migrating cranial NC cells in the forebrain and hindbrain as early as the 7-somite stage and reaches its peak expression at the 14-somite stage. Additionally, *P0-Cre* labels notochord at the 4–7 somite stages in early embryos. Moreover, the distribution pattern of *P0-Cre* was different from *Wnt1-Cre* in labeling NC cells, especially in the midbrain and hindbrain regions. Our data indicate that the *P0-Cre* mouse line is a valuable model for studies of NC and notochord lineage, and that careful attention needs to be paid in choosing promoters to drive Cre and its reporters for studies on NC lineage in early embryos.

AUTHOR CONTRIBUTION

Experimental design: GC, MI, JY, SC, YK, YM and HXL. Experiment conduction and data analysis: GC, MI, JY, SK, TF, GS, MKR, CS, YK, YM and HXL. Data interpretation: GC, YK, YM and HXL. Writing manuscript: GC, YM and HXL. Approving final version of manuscript: GC, MI, JY, SK, TF, GS, MKR, CS, SC, YK, YM and HXL. HXL and YM take responsibility for the integrity of the data analysis.

REFERENCE

Aoto, K., Sandell, L. L., Butler Tjaden, N. E., Yuen, K. C., Watt, K. E., Black, B. L., . . . Trainor, P. A. (2015). Mef2c-F10N enhancer driven beta-galactosidase (LacZ) and Cre recombinase mice facilitate analyses of gene function and lineage fate in neural crest cells. *Developmental Biology, 402*, 3–16.

Araki, K., Araki, M., Miyazaki, J., & Vassalli, P. (1995). Site-specific recombination of a transgene in fertilized eggs by transient expression of Cre recombinase. *Proceedings of the National Academy of Science of United States of America, 92*, 160–164.

Barriga, E. H., Trainor, P. A., Bronner, M., & Mayor, R. (2015). Animal models for studying neural crest development: Is the mouse different? *Development, 142*, 1555–1560.

Boggs, K., Venkatesan, N., Mederacke, I., Komatsu, Y., Stice, S., Schwabe, R. F., . . . Liu, H. X. (2016). Contribution of underlying connective tissue cells to taste buds in mouse tongue and soft palate. *PLoS One, 11*, e0146475.

Bronner-Fraser, M. (2004). Development. Making sense of the sensory lineage. *Science, 303*, 966–968.

Cavanaugh, A. M., Huang, J., & Chen, J. N. (2015). Two developmentally distinct populations of neural crest cells contribute to the zebrafish heart. *Developmental Biology, 404*, 103–112.

Chai, Y., Jiang, X., Ito, Y., Bringas, P., Jr., Han, J., Rowitch, D. H., . . . Sucov, H. M. (2000). Fate of the mammalian cranial neural crest during tooth and mandibular morphogenesis. *Development, 127*, 1671–1679.

Chai, Y., & Maxson, R. E. Jr. (2006). Recent advances in craniofacial morphogenesis. *Dev Dyn, 235*, 2353–2375.

Chan, W. Y., & Tam, P. P. (1988). A morphological and experimental study of the mesencephalic neural crest cells in the mouse embryo using wheat germ agglutinin-gold conjugate as the cell marker. *Development, 102*, 427–442.

Crane, J. F., & Trainor, P. A. (2006). Neural crest stem and progenitor cells. *Annual Reviews of Cell Developmental Biology, 22*, 267–286.

Danielian, P. S., Muccino, D., Rowitch, D. H., Michael, S. K., & McMahon, A. P. (1998). Modification of gene activity in mouse embryos in utero by a tamoxifen-inducible form of Cre recombinase. *Current Biology, 8*, 1323–1326.

Echelard, Y., Vassileva, G., & McMahon, A. P. (1994). *Cis*-acting regulatory sequences governing Wnt-1 expression in the developing mouse CNS. *Development, 120*, 2213–2224.

Feltri, M. L., D'antonio, M., Previtali, S., Fasolini, M., Messing, A., & Wrabetz, L. (1999a). P0-Cre transgenic mice for inactivation of adhesion molecules in Schwann cells. *Annals of New York Academy of Science, 883*, 116–123.

Feltri, M. L., D'antonio, M., Quattrini, A., Numerato, R., Arona, M., Previtali, S., . . . Wrabetz, L. (1999b). A novel P0 glycoprotein transgene activates expression of lacZ in myelin-forming Schwann cells. *European Journal of Neuroscience, 11*, 1577–1586.

Freem, L. J., Escot, S., Tannahill, D., Druckenbrod, N. R., Thapar, N., & Burns, A. J. (2010). The intrinsic innervation of the lung is derived from neural crest cells as shown by optical projection tomography in Wnt1-Cre;YFP reporter mice. *Journal of Anatomy, 217*, 651–664.

Freyer, L., Aggarwal, V., & Morrow, B. E. (2011). Dual embryonic origin of the mammalian otic vesicle forming the inner ear. *Development, 138*, 5403–5414.

Gershon, T. R., Shiraz, A., Qin, L. X., Gerald, W. L., Kenney, A. M., & Cheung, N. K. (2009). Enteric neural crest differentiation in ganglioneuromas implicates Hedgehog signaling in peripheral neuroblastic tumor pathogenesis. *PLoS One*, 4, e7491.

Hu, N., Strobl-Mazzulla, P. H., & Bronner, M. E. (2014). Epigenetic regulation in neural crest development. *Developmental Biology*, 396, 159–168.

Huang, T., Liu, Y., Huang, M., Zhao, X., & Cheng, L. (2010). Wnt1-cre-mediated conditional loss of Dicer results in malformation of the midbrain and cerebellum and failure of neural crest and dopaminergic differentiation in mice. *Journal of Molecular Cell Biology*, 2, 152–163.

Ikeya, M., Lee, S. M., Johnson, J. E., McMahon, A. P., & Takada, S. (1997). Wnt signalling required for expansion of neural crest and CNS progenitors. *Nature*, 389, 966–970.

Jarad, G., & Miner, J. H. (2009). The Pax3-Cre transgene exhibits a rostrocaudal gradient of expression in the skeletal muscle lineage. *Genesis*, 47, 1–6.

Jiang, X., Iseki, S., Maxson, R. E., Sucov, H. M., & Morriss-Kay, G. M. (2002). Tissue origins and interactions in the mammalian skull vault. *Developmental Biology*, 241, 106–116.

Jinno, H., Morozova, O., Jones, K. L., Biernaskie, J. A., Paris, M., Hosokawa, R., ... Miller, F. D. (2010). Convergent genesis of an adult neural crest-like dermal stem cell from distinct developmental origins. *Stem Cells*, 28, 2027–2040.

Jurand, A. (1974). Some aspects of the development of the notochord in mouse embryos. *Journal of Embryology & Experimental Morphology*, 32, 1–33.

Katoh, H., Shibata, S., Fukuda, K., Sato, M., Satoh, E., Nagoshi, N., ... Okano, H. (2011). The dual origin of the peripheral olfactory system: Placode and neural crest. *Molecular Brain*, 4, 34.

Kawakami, M., Umeda, M., Nakagata, N., Takeo, T., & Yamamura, K. (2011). Novel migrating mouse neural crest cell assay system utilizing P0-Cre/EGFP fluorescent time-lapse imaging. *BMC Developmental Biology*, 11, 68.

Kawamoto, S., Niwa, H., Tashiro, F., Sano, S., Kondoh, G., Takeda, J., ... Miyazaki, J. (2000). A novel reporter mouse strain that expresses enhanced green fluorescent protein upon Cre-mediated recombination. *FEBS Letters*, 470, 263–268.

Komatsu, Y., Yu, P. B., Kamiya, N., Pan, H., Fukuda, T., Scott, G. J., ... Mishina, Y. (2013). Augmentation of Smad-dependent BMP signaling in neural crest cells causes craniosynostosis in mice. *Journal of Bone & Mineral Research*, 28, 1422–1433.

Lee, R. T., Nagai, H., Nakaya, Y., Sheng, G., Trainor, P. A., Weston, J. A., & Thiery, J. P. (2013). Cell delamination in the mesencephalic neural fold and its implication for the origin of ectomesenchyme. *Development*, 140, 4890–4902.

Leikola, A. (1976). The neural crest: migrating cells in embryonic development. *Folia Morphology (Praha)*, 24, 155–172.

Lewis, A. E., Vasudevan, H. N., O'neill, A. K., Soriano, P., & Bush, J. (2013). The widely used Wnt1-Cre transgene causes developmental phenotypes by ectopic activation of Wnt signaling. *Developmental Biology*, 379, 229–234.

Li, Z., Xie, W. B., Escano, C. S., Asico, L. D., Xie, Q., Jose, P. A., & Chen, S. Y. (2011). Response gene to complement 32 is essential for fibroblast activation in renal fibrosis. *Journal of Biological Chemistry*, 286, 41323–41330.

Liu, H. X., Komatsu, Y., Mishina, Y., & Mistretta, C. M. (2012). Neural crest contribution to lingual mesenchyme, epithelium and developing taste papillae and taste buds. *Developmental Biology*, 368, 294–303.

Liu, Y., & Xiao, A. (2011). Epigenetic regulation in neural crest development. *Birth Defects Research Part A: Clinical & Molecular Teratology*, 91, 788–796.

McCann, M. R., Tamplin, O. J., Rossant, J., & Seguin, C. A. (2012). Tracing notochord-derived cells using a Noto-cre mouse: implications for intervertebral disc development. *Disease Models & Mechanisms*, 5, 73–82.

McMahon, A. P., Joyner, A. L., Bradley, A., & McMahon, J. A. (1992). The midbrain-hindbrain phenotype of Wnt-1-/Wnt-1- mice results from stepwise deletion of engrailed-expressing cells by 9.5 days postcoitum. *Cell*, 69, 581–595.

Menendez, L., Yatskievych, T. A., Antin, P. B., & Dalton, S. (2011). Wnt signaling and a Smad pathway blockade direct the differentiation of human pluripotent stem cells to multipotent neural crest cells. *Proceedings of the National Academy of Science of United States of America*, 108, 19240–19245.

Meulemans, D., & Bronner-Fraser, M. (2004). Gene-regulatory interactions in neural crest evolution and development. *Developmental Cell*, 7, 291–299.

Milgrom-Hoffman, M., Michailovici, I., Ferrara, N., Zelzer, E., & Tzahor, E. (2014). Endothelial cells regulate neural crest and second heart field morphogenesis. *Biology Open*, 3, 679–688.

Mori-Akiyama, Y., Akiyama, H., Rowitch, D. H., & de Crombrugghe, B. (2003). Sox9 is required for determination of the chondrogenic cell lineage in the cranial neural crest. *Proc Natl Acad Sci U S A*, 100, 9360–9365.

Morikawa, S., Mabuchi, Y., Niibe, K., Suzuki, S., Nagoshi, N., Sunabori, T., ... Matsuzaki, Y. (2009). Development of mesenchymal stem cells partially originate from the neural crest. *Biochemical & Biophysical Research Communications*, 379, 1114–1119.

Munoz, W. A., & Trainor, P. A. (2015). Neural crest cell evolution: how and when did a neural crest cell become a neural crest cell. *Current Topics in Developmental Biology*, 111, 3–26.

Nagoshi, N., Shibata, S., Hamanoue, M., Mabuchi, Y., Matsuzaki, Y., Toyama, Y., ... Okano, H. (2011). Schwann cell plasticity after spinal cord injury shown by neural crest lineage tracing. *Glia*, 59, 771–784.

Nagoshi, N., Shibata, S., Kubota, Y., Nakamura, M., Nagai, Y., Satoh, E., ... Okano, H. (2008). Ontogeny and multipotency of neural crest-derived stem cells in mouse bone marrow, dorsal root ganglia, and whisker pad. *Cell Stem Cell*, 2, 392–403.

Nakamura, T., Colbert, M. C., & Robbins, J. (2006). Neural crest cells retain multipotential characteristics in the developing valves and label the cardiac conduction system. *Circulation Research*, 98, 1547–1554.

Nakanishi, K., Chan, Y. S., & Ito, K. (2007). Notch signaling is required for the chondrogenic specification of mouse mesencephalic neural crest cells. *Mechanisms of Development*, 124, 190–203.

Nichols, D. H. (1981). Neural crest formation in the head of the mouse embryo as observed using a new histological technique. *Journal of Embryology & Experimental Morphology*, 64, 105–120.

Noden, D. M., & Trainor, P. A. (2005). Relations and interactions between cranial mesoderm and neural crest populations. *Journal of Anatomy*, 207, 575–601.

Nomura-Kitabayashi, A., Phoon, C. K., Kishigami, S., Rosenthal, J., Yamauchi, Y., Abe, K., ... Mishina, Y. (2009). Outflow tract cushions perform a critical valve-like function in the early embryonic heart requiring BMPRIA-mediated signaling in cardiac neural crest. *American Journal of Physiology: Heart & Circulatory Physiology*, 297, H1617–H1628.

Novak, A., Guo, C., Yang, W., Nagy, A., & Lobe, C. G. (2000). Z/EG, a double reporter mouse line that expresses enhanced green fluorescent protein upon Cre-mediated excision. *Genesis*, 28, 147–155.

Ogawa, Y., Eto, A., Miyake, C., Tsuchida, N., Miyake, H., Takaku, Y., ... Oishi, K. (2015). Induced pluripotent stem cells generated from P0-Cre;Z/EG transgenic mice. *PLoS One*, 10, e0138620.

Ono, M., Suzawa, T., Takami, M., Yamamoto, G., Hosono, T., Yamada, A., ... Kamijo, R. (2015). Localization and osteoblastic differentiation potential of neural crest-derived cells in oral tissues of adult mice. *Biochemical & Biophysical Research Communication 464*, 1209–1214.

Pomp, O., Brokhman, I., Ben-Dor, I., Reubinoff, B., & Goldstein, R. S. (2005). Generation of peripheral sensory and sympathetic neurons and neural crest cells from human embryonic stem cells. *Stem Cells, 23*, 923–930.

Rowitch, D. H., Echelard, Y., Danielian, P. S., Gellner, K., Brenner, S., & McMahon, A. P. (1998). Identification of an evolutionarily conserved 110 base-pair cis-acting regulatory sequence that governs Wnt-1 expression in the murine neural plate. *Development, 125*, 2735–2746.

Sahar, D. E., Longaker, M. T., & Quarto, N. (2005). Sox9 neural crest determinant gene controls patterning and closure of the posterior frontal cranial suture. *Developmental Biology, 280*, 344–361.

Sakai, K., & Miyazaki, J. (1997). A transgenic mouse line that retains Cre recombinase activity in mature oocytes irrespective of the cre transgene transmission. *Biochemical & Biophysical Research Communication, 237*, 318–324.

Serbedzija, G. N., Bronner-Fraser, M., & Fraser, S. E. (1992). Vital dye analysis of cranial neural crest cell migration in the mouse embryo. *Development, 116*, 297–307.

Simon, C., Lickert, H., Gotz, M., & Dimou, L. (2012). Sox10-iCreERT2: a mouse line to inducibly trace the neural crest and oligodendrocyte lineage. *Genesis, 50*, 506–515.

Sommer, L., & Suter, U. (1998). The glycoprotein P0 in peripheral gliogenesis. *Cell Tissue Research, 292*, 11–16.

Soriano, P. (1999). Generalized lacZ expression with the RoSA26 Cre reporter strain. *Nature Genetics, 21*, 70–71.

Spokony, R. F., Aoki, Y., Saint-Germain, N., Magner-Fink, E., & Saint-Jeannet, J. P. (2002). The transcription factor Sox9 is required for cranial neural crest development in Xenopus. *Development, 129*, 421–432.

Suzuki, J., Yoshizaki, K., Kobayashi, T., & Osumi, N. (2013). Neural crest-derived horizontal basal cells as tissue stem cells in the adult olfactory epithelium. *Neuroscience Research, 75*, 112–120.

Tallquist, M. D., & Soriano, P. (2000). Epiblast-restricted Cre expression in MoRE mice: a tool to distinguish embryonic vs. extra-embryonic gene function. *Genesis, 26*, 113–115.

Tomita, Y., Matsumura, K., Wakamatsu, Y., Matsuzaki, Y., Shibuya, I., Kawaguchi, H., ... Fukuda, K. (2005). Cardiac neural crest cells contribute to the dormant multipotent stem cell in the mammalian heart. *Journal of Cell Biology, 170*, 1135–1146.

Trainor, P. A. (2005a). Specification and patterning of neural crest cells during craniofacial development. *Brain, Behavior, & Immunity, 66*, 266–280.

Trainor, P. A. (2005b). Specification of neural crest cell formation and migration in mouse embryos. *Seminars in Cell & Developmental Biology, 16*, 683–693.

Trainor, P. A. (2015). Neural crest and placodes. Preface. *Current Topics in Developmental Biology, 111*, 15–16.

Wang, S. K., Komatsu, Y., & Mishina, Y. (2011). Potential contribution of neural crest cells to dental enamel formation. *Biochemical & Biophysical Research Communications, 415*, 114–119.

Wang, Q., Kumar, S., Mitsios, N., Slevin, M., & Kumar, P. (2007). Investigation of downstream target genes of PAX3c, PAX3e and PAX3g isoforms in melanocytes by microarray analysis. *International Journal of Cancer, 120*, 1223–1231.

Weissman, T. A., & Pan, Y. A. (2015). Brainbow: New resources and emerging biological applications for multicolor genetic labeling and analysis. *Genetics, 199*, 293–306.

Weissman, T. A., Sanes, J. R., Lichtman, J. W., & Livet, J. (2011). Generation and imaging of Brainbow mice. *Cold Spring Harbor Protocols, 2011*, 851–856.

Yamauchi, Y., Abe, K., Mantani, A., Hitoshi, Y., Suzuki, M., Osuzu, F., ... Yamamura, K. (1999). A novel transgenic technique that allows specific marking of the neural crest cell lineage in mice. *Developmental Biology, 212*, 191–203.

Yoshida, S., Shimmura, S., Nagoshi, N., Fukuda, K., Matsuzaki, Y., Okano, H., & Tsubota, K. (2006). Isolation of multipotent neural crest-derived stem cells from the adult mouse cornea. *Stem Cells, 24*, 2714–2722.

Yoshida, T., Vivatbutsiri, P., Morriss-Kay, G., Saga, Y., & Iseki, S. (2008). Cell lineage in mammalian craniofacial mesenchyme. *Mechanisms of Development, 125*, 797–808.

Young, H. M. (2000). Increased expression of p75NTR by neural crest-derived cells in vivo during mitosis. *Neuroreport, 11*, 725–728.

Young, H. M., Ciampoli, D., Hsuan, J., & Canty, A. J. (1999). Expression of Ret-, p75(NTR)-, Phox2a-, Phox2b-, and tyrosine hydroxylase-immunoreactivity by undifferentiated neural crest-derived cells and different classes of enteric neurons in the embryonic mouse gut. *Developmental Dynamics, 216*, 137–152.

Zhang, S. M., Marsh, R., Ratner, N., & Brackenbury, R. (1995). Myelin glycoprotein P0 is expressed at early stages of chicken and rat embryogenesis. *Journal of Neuroscience Research, 40*, 241–250.

SUPPORTING INFORMATION

Additional Supporting Information may be found in the online version of this article.